



Published in final edited form as:

J Med Chem. 2017 June 08; 60(11): 4680–4692. doi:10.1021/acs.jmedchem.7b00304.

Pyrazolopyrimidines as Potent Stimulators for Transient Receptor Potential Canonical 3/6/7 Channels

Chunrong Qu[†], Mingmin Ding[†], Yingmin Zhu[‡], Yungang Lu[‡], Juan Du[§], Melissa Miller^{||,+}, Jinbin Tian[‡], Jinmei Zhu[†], Jian Xu^{⊥,#}, Meng Wen[†], AGA Er-Bu[○], Jule Wang[○], Yuling Xiao[†], Meng Wu[●], Owen B. McManus^{||,°}, Min Li[■], Jilin Wu^{#,▽}, Huai-Rong Luo^{◆,&}, Zhengyu Cao[⊥], Bing Shen[§], Hongbo Wang^{*,¶}, Michael X. Zhu^{*,‡,#}, and Xuechuan Hong^{*,†,○}

[†]State Key Laboratory of Virology, Key Laboratory of Combinatorial Biosynthesis and Drug Discovery (MOE) and Hubei Province Engineering and Technology Research Center for Fluorinated Pharmaceuticals, Wuhan University School of Pharmaceutical Sciences, Wuhan, Hubei Province 430071, China

[‡]Department of Integrative Biology and Pharmacology, McGovern Medical School, The University of Texas Health Science Center at Houston, Houston, Texas 77030, United States

[§]School of Basic Medical Sciences, Anhui Medical University, Hefei, Anhui Province 230032, China

^{||}Department of Neuroscience, High Throughput Biology Center and Johns Hopkins Ion Channel Center, Johns Hopkins University School of Medicine, Baltimore, Maryland 21205, United States

[⊥]State Key Laboratory of Natural Medicines, Jiangsu Provincial Key laboratory for TCM Evaluation and Translational Development, China Pharmaceutical University, Nanjing, Jiangsu Province 211198, China

[#]The International Scientist Working Station of Neuropharmacology, Shanghai Institute of Materia Medica, Chinese Academy of Sciences, Shanghai, 201203, China

*Corresponding Authors: For X. Hong (lead contact): phone, 86-027-68752331; xhy78@whu.edu.cn. For H. Wang: hongbowangyt@gmail.com. For M. X. Zhu: michael.x.zhu@uth.tmc.edu.

[†]For M. Miller: University of California at Berkeley, Berkeley, California 94720, United States.

[●]For M. Wu: High-Throughput Screening Facility, University of Iowa, Iowa City, Iowa 52242, United States.

[°]For O. B. McManus: Essen Bioscience, Ann Arbor, Michigan 48108 United States.

[■]For M. Li: GlaxoSmithKline, Philadelphia, Pennsylvania 19103, United States.

[&]For H. Luo: Southwest Medical University, Luzhou, Sichuan 646000, China.

ORCID

Xuechuan Hong: 0000-0001-6834-3278

Author Contributions

Chunrong Qu, Mingmin Ding, and Yingmin Zhu contributed equally to this work. X. Hong, M. X. Zhu, M. Li, B. Shen, Z. Cao, H. Wang, and H. R. Luo designed the research; C. Qu, M. Ding, Y. Zhu, Y. Lu, J. Zhu, J. Du, M. Miller, J. Tian, J. Xu, M. Wen, M. Wu, and J. Wu performed experiments; X. Hong, M. X. Zhu, H. Wang, C. Qu, M. Ding, Y. Lu, Y. Xiao, O. B. McManus, and J. Wang performed data analyses; M. Ding and AGA Er-Bu performed HPLC analyses; X. Hong, M. X. Zhu, H. Wang, C. Qu, M. Ding, Y. Lu, and H. R. Luo wrote the paper.

Notes

The authors declare no competing financial interest.

Supporting Information

The Supporting Information is available free of charge on the ACS Publications website at DOI: 10.1021/acs.jmed-chem.7b00304.

¹H NMR spectral information for compounds **6a–6c**, **7a–7b**, **8a–8d**, **11a–11c**; ¹H NMR and ¹³C NMR spectral information for compounds **4a–4p**; HPLC results and HPLC traces information for compounds **4a–4p** (PDF)

Molecular formula strings (CSV)

▽University of Chinese Academy of Sciences, Beijing, 100049, China

○Medical College, Tibet University, Lasa, Tibet 850000, China

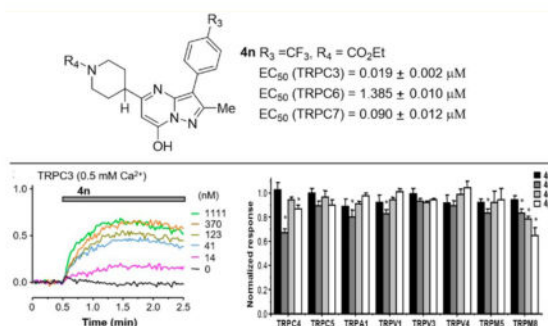
◆Key Laboratory of Phytochemistry and Plant Resources in West China, Kunming Institute of Botany, Chinese Academy of Sciences, Kunming, Yunnan Province 650201, China

¶School of Pharmacy, Key Laboratory of Molecular Pharmacology and Drug Evaluation (Yantai University), Ministry of Education, Yantai University, Yantai, Shangdong Province 264005, China

Abstract

Transient receptor potential canonical 3/6/7 (TRPC3/6/7) are highly homologous receptor-operated non-selective cation channels. Despite their physiological significance, very few selective and potent agonists are available for functional examination of these channels. Using a cell-based high throughput screening approach, a lead compound with the pyrazolopyrimidine skeleton was identified as a TRPC6 agonist. Synthetic schemes for the lead and its analogues were established, and structural–activity relationship studies were carried out. A series of potent and direct agonists of TRPC3/6/7 channels were identified, and among them, **4m–4p** have a potency order of TRPC3 > C7 > C6, with **4n** being the most potent with an EC₅₀ of <20 nM on TRPC3. Importantly, these compounds exhibited no stimulatory activity on related TRP channels. The potent and selective compounds described here should be suitable for evaluation of the roles of TRPC channels in the physiology and pathogenesis of diseases, including glomerulosclerosis and cancer.

Graphical Abstract



INTRODUCTION

Transient receptor potential canonical (TRPC) channels constitute a group of receptor-operated calcium-permeable nonselective cation channels of the TRP superfamily. The seven mammalian TRPC members can be further divided into four subgroups (TRPC1, TRPC2, TRPC4/5, and TRPC3/6/7) based on their amino acid sequences and functional similarities.¹ Native TRPC channels may be formed of either homo- or heterotetramers from the same subgroup or from different subgroups; they also interact with a variety of other proteins, which exert modulatory roles on their assembly, trafficking, and/or function.² So far, the majority of studies on TRPC channels have focused on their roles in mediating Ca²⁺ and Na⁺ influx after the stimulation of phospholipase C (PLC) either by G protein-coupled

receptors that signal through the $G_{q/11}$ subgroup of heterotrimeric G proteins or by receptor tyrosine kinases.³ These activities cause membrane depolarization and a sustained increase in intracellular Ca^{2+} concentration ($[Ca^{2+}]_i$), which are important for a plethora of cellular functions in many physiological systems.⁴ On the other hand, a few studies also implicated TRPC channel expression and function in intracellular membranes,⁵ suggesting that very diverse cellular activities may be regulated by these channels.

Intensive investigations have been instrumental in defining the physiological roles of TRPC channels in different tissues and organs, including excitation–contraction coupling in smooth muscles,^{6,7} protein filtration in the kidney,^{8,9} synaptic formation and transmission,^{10,11} myofibroblast transdifferentiation and wound healing,¹² regulation of vascular tone, and cell growth and proliferation.^{13–15} Particularly, TRPC6 has been implicated in the physiological regulation of glomerular hemodynamics in kidney. Genetic mutations of TRPC6, including both gain-of-function and loss-of-function ones, have been linked to glomerular dysfunction in the kidney, where the channel is expressed in podocytes and involved in the regulation of slit diaphragm for protein filtration.^{8,9,16} Elevated expression of TRPC6 was found in glomeruli from patients with proteinuria, which is a common feature of kidney dysfunction of glomerular origin and is by itself a risk factor for both renal and extrarenal diseases.¹⁷ Additionally, TRPC6 and its closely related TRPC3, are both suggested to be involved in the development of cardiac hypertrophy and hypertension.^{14,18–20} The roles for TRPC3/6 in cancer have also been suggested.^{21,22} However, the exact roles played by TRPC channels in kidney and cardiovascular functions and the underlying mechanisms concerning how they contribute to these functions and/or pathogenesis have proven difficult to elucidate due to the lack of specific compounds that modulate these channels.

TRPC3, TRPC6, and TRPC7 are closely related, sharing 65–78% sequence identity, and form channels that are generally activated downstream from receptors that activate PLC. These channels are also directly activated by diacylglycerols (DAG), one of the products of phosphatidylinositol 4,5-bisphosphate (PIP_2) hydrolysis by PLC.^{23,24} Analogues of DAG, such as 1-oleoyl-2-acetyl-*sn*-glycerol (**1**) (OAG) and 1,2-dioctanoyl-*sn*-glycerol (**2**) (DOG) have been widely used to activate TRPC3 and TRPC6 channels (Figure 1). However, not only are these stimulators nonspecific for TRPC3/6/7 channels, but also they are highly hydrophobic and unstable in the aqueous solution. Recently, small molecular probes, including both natural products and synthetic compounds, have been reported for TRPC channels. For example, a novel synthetic agonist for TRPC3/6 named GSK1702934A (**3**)²⁵ was used at 1 μM to study cardiac contractility and arrhythmogenesis in heart.²⁶ A few small-molecule compounds including Pyr3 and analogues,²⁷ cationic, *N*'-substituted 1-benzylpiperidines,⁷ anilino-thiazole,²⁸ norges-timate,²⁹ 4-((1*R*,2*R*)-2-[(3*R*)-3-aminopiperidin-1-yl]-2,3-dihydro-1*H*-inden-1-yl)oxy)-3-chlorobenzonitrile,³⁰ and larixyl acetate³¹ have been identified as inhibitors of TRPC3/6/7 channels. Englerin A,³² riluzole,³³ clemizole hydrochloride,³⁴ 4-methyl-2-(1-piperidinyl)-quinoline (ML204),³⁵ and 2-amino-benzimidazole derivatives³⁶ have been described as TRPC4 and/or TRPC5 agonists or antagonists. Often, these probes cross-react within the subgroup of TRPC3/6/7 or TRPC4/5 but not between the two subgroups.

While selectivity remains lacking for most compounds, identification of their pharmacophores through systematic structure–activity approaches can be expected to lead to development of subtype-selective TRPC agonists or antagonists and may perhaps lead to development of novel drug therapies such as for the treatment of kidney and cardiovascular diseases or cancer. For such a reason, we have carried out a high-throughput screening (HTS) effort to identify small-molecule probes of TRPC6 and related channels as a starting point for lead optimization and target validation. Here, we report the identification of a novel pyrazolopyrimidine-based TRPC6 lead agonist, its resynthesis, and the structure–activity relationship (SAR) analysis of the initial set of its analogues on TRPC3, TRPC6, and TRPC7. With minor modifications, we obtained an agonist with relatively strong selectivity for TRPC3, exhibiting apparent affinity at the low nanomolar range.

RESULTS AND DISCUSSION

Chemistry

The scarcity of TRPC3/6/7 probes has severely hampered the characterization of these channels in their assembly, function, and pathophysiological roles. To functionally screen for TRPC3/6/7 small molecular probes, we created a stable HEK293 cell line that coexpressed mouse TRPC6 and the $G_{q/11}$ -PLC β coupled M5 muscarinic receptor (TRPC6 cells). These cells responded to the muscarinic agonist, carbachol (CCh), with a strong sustained membrane depolarization, which can be detected by the FLIPR membrane potential (FMP) dye as an increase in fluorescence (Figure 2A, gray dashed line). Using this cell-based assay, we screened 305000 compounds from the Molecular Libraries Small Molecule Repository (MLSMR), supported by the Molecular Libraries Probe Production Centers Network (MLPCN) and identified an activator with the pyrazolopyrimidine skeleton (PubChem CID: 5308428, Table 1, compound **4o**) as the primary hit. As shown in Figure 2A, the original lead compound elicited membrane potential depolarization in TRPC6 cells in a concentration-dependent manner but not in the parental HEK293 cells (Figure 2B). It also evoked $[Ca^{2+}]_i$ rise in the TRPC6 cells (Figure 2C) but not parental HEK293 cells (Figure 2D). We then confirmed that the compound concentration dependently elicited half maximal stimulation (EC_{50}) were estimated to be $1.4 \pm 0.1 \mu M$ by the FMP assay ($n = 6$), $2.5 \pm 0.2 \mu M$ (at +80 mV) by whole-cell recordings ($n = 5-7$), and $7.2 \pm 0.5 \mu M$ by the Ca^{2+} assay ($n = 12$) (Figure 2F).

To further evaluate this compound and the SAR on TRPC6 activation, we first synthesized compounds **4a–4p** (Scheme 1, Table 1). Starting from the commercially available piperidine-4-carboxylic acid **5**, our initial attempt to introduce a methyl group or alkyl group into the R_1 position did not work until a published protocol³⁸ was adapted to protect the carboxyl group before adding methyl at position R_1 . Using this strategy, compounds **6a–6c** were prepared with high yields of 90–95% by *N*-acylation with ethyl chloroformate, di-*tert*-butyl dicarbonate, or benzyl chloroformate groups at position R_2 , respectively (Scheme 1). deprotonation of piperidine of **6a** and **6b** with 1.2 equiv of *n*-butyllithium followed by reaction with methyl iodide afforded amides **7a** and **7b** in 87% and 85% yields, respectively. The ethyl ester portion of **7a** and **7b** was converted to 3-oxopropanoate group using a modified Masamune procedure,³⁹ which furnished β -keto esters **8a** and **8b** in 82% and 86%

yields, respectively. Compounds **8c** and **8d** were obtained with high yields from **6c** and **6b**, respectively, using a similar procedure. Condensation of nitrile intermediate **10** with 1,1-dimethoxy-*N,N*-dimethylethan-1-amine (**9**) using dichloromethane as the solvent under microwave irradiation (MWI), followed by the cyclization reaction with hydrazine hydrochloride in EtOH, generated the 5-aminopyrazoles **11a–d** in excellent yields (81–88%) over two steps. We then carried out a cyclization study of compounds **8** and **11** using a variety of acids, such as HCl, trifluoroacetic acid (TFA), and H₂SO₄, in order to test the viability of our design. Unfortunately, only a trace amount of product **12** was formed in TFA at reflux for 18 h. However, mixing **8a–8c** with **11a–11d** in acetic acid in a microwave reactor at 120 °C overnight produced the desired products **12** in good yields. Deprotection of the Boc group of compounds **12** (R₂ = Boc) with TFA/dichloromethane (DCM) at 0 °C resulted in the formation of compounds **13** in high yield. Finally, amidation of compounds **13** gave rise to compounds **4** (**4a–4p**, Table 1) successfully (Scheme 1).

Biological Evaluation

The effect of the newly synthesized compounds (Table 1) on TRPC6 channel function was evaluated using the fluorescence Ca²⁺ assay. As the original lead, the resynthesized compound **4o** (R₁ = H, R₃ = F, R₄ = CO₂Et) evoked [Ca²⁺]_i rise in the TRPC6 cells in a concentration dependent manner, with a mean EC₅₀ value of 4.66 ± 0.03 μM (Figure 2C,E, Table 1, entry 15), demonstrating a comparable activity of the resynthesized compound on TRPC6 as the original lead. Compound **4o** was also tested on HEK293 cells that coexpressed μ opioid receptor (MOR) and TRPC4β,^{35,36} which belongs to a different subgroup of TRPC channels than TRPC3/6/7. Upon stimulation by a μ agonist, (D-Ala, *N*-MePhe, Gly-ol]-enkephalin (DAMGO, 1 μM), these cells show a robust increase in [Ca²⁺]_i.³⁶ However, compound **4o** did not elicit a Ca²⁺ response in the MOR/TRPC4β cells, nor did it alter the DAMGO-evoked response, demonstrating its selectivity for TRPC6 over TRPC4.

We next investigated SAR between substituents in R₁ and R₄ of ring A and R₃ of ring B using the Ca²⁺ assay on the TRPC6 cells (Table 1). For most compounds, the MOR/TRPC4β cells were used as a control for subtype selectivity. First, the hydrogen is required in R₁, as the substitution by a methyl group rendered all compounds (**4b–4h**) inactive at stimulating TRPC6 (Table 1, entries 2–8), except for **4g**, which, however, showed high fluorescence by the compound itself (not shown). This could be due in part to the ability of methyl at position R₁ to bias a particular A ring conformer. Second, the substitution of F at R₃ by Cl moderately increased the EC₅₀ (**4m**, Figure 3A,E, Table 1, entry 13), whereas that by NO₂ or CF₃ decreased the EC₅₀ by ~60–70% to 2 μM (**4i** and **4n**, Figure 3B,E, Table 1, entries 9 and 14), suggesting a possible position for further modifications to improve the agonist potency. However, like **4g**, the introduction of NO₂ at R₃ rendered the compound (**4i**) to become self-fluorescent (not shown). Third, substitutions at R₄ of the A ring revealed that the carbamate group, such as ethyl carbamate, is optimal. To identify suitable carbamate group replacements for R₄, we used 6-bromo-nicotine (**4a**), ethyl carbamoyl (**4j**), *tert*-butyloxycarbonyl (Boc, **4l**), and carboxybenzyl (Cbz, **4m**, **4p**). Intriguingly, compound **4l** did not exhibit stimulatory activity on TRPC6, likely because of the steric hindrance blockade by the Boc group introduced at the R₄ position. The benzyl carbamate or Cbz

group in R₄ (**4p**) displayed comparable stimulatory activity on TRPC6 as the corresponding ethyl carbamate (**4o**), giving an EC₅₀ value of $3.91 \pm 0.02 \mu\text{M}$ (Figure 3D,E, Table 1, entry 16).

Functional Characterization of 4m–4p

To validate the agonistic action of pyrazolopyrimidine compounds on TRPC6 channels, we focused on the last four compounds listed in Table 1 (**4m–4p**), which evoked robust $[\text{Ca}^{2+}]_i$ increases in TRPC6-expressing cells in the Ca²⁺ assay with EC₅₀ values $<8 \mu\text{M}$ (Figure 3A–E) and no self-fluorescence. In whole-cell voltage clamp recordings, we used a low Ca²⁺ bath solution (0.1 mM Ca²⁺) in order to minimize current rundown. Under these conditions, increasing concentrations (0.1–100 μM) of the test compound were applied consecutively, and in each case the compound evoked stepwise current increases in individual cells at both negative and positive potentials (Figure 3F–I). Noticeably, the outward currents at positive potentials developed earlier at low compound concentrations than the inward currents at negative potentials, indicative of a shift of voltage dependence as the compound concentration increased. Typically, the currents did not desensitize even at highest concentrations (20–100 μM) used. On the basis of the currents at +80 mV, the EC₅₀ values for monovalent cation currents of TRPC6 evoked by **4m–4p** were determined to be 2.05 ± 0.02 , 0.89 ± 0.01 , 6.28 ± 0.02 , and $3.24 \pm 0.01 \mu\text{M}$ ($n = 6–8$), respectively (Figure 3J). These values are comparable to that obtained from the Ca²⁺ assay (Table 1).

We then examined whether the compounds directly activate closely related TRPC3 and TRPC7 channels. Although our initial attempts using the FMP and Ca²⁺ assays did not reveal obvious activation of human TRPC3 stably expressed in HEK293 cells by compound **4o** (Figure 4A₁,A₂), lowering the Ca²⁺ concentration in the extracellular solution from the standard 2 mM to 0.5 mM allowed **4o** to evoke membrane depolarization in these cells in a concentration-dependent manner (Figure 4B). These results suggest that the activation of TRPC3 by **4o** is sensitive to inhibition by extracellular Ca²⁺, consistent with the previous finding that physiological concentrations of extracellular Ca²⁺ suppressed receptor-operated TRPC3 currents.⁴⁰ Supporting the FMP assay data, **4o** also evoked whole-cell currents in HEK293 cells that expressed human TRPC3 (Figure 4E). Using the FMP assay with 0.5 mM extracellular Ca²⁺, we determined the EC₅₀ values of compounds **4m–4p** on stimulating TRPC3 to be 138 ± 23 , 19.2 ± 2.3 , 450 ± 87 , and $236 \pm 47 \text{ nM}$ (Figure 4B–D, $n = 6$ for each), respectively. Among the four analogues, **4n** really stands out, exhibiting >7 -fold increase in the potency on TRPC3 as compared to other compounds and >70 -fold increase as compared to the same compound on TRPC6.

Among the three members of the TRPC3/6/7 subgroup, the sequence of TRPC7 is more similar to TRPC3 than to TRPC6. Interestingly, compound **4o** was able to elicit membrane depolarization and $[\text{Ca}^{2+}]_i$ elevation in HEK293 cells that stably expressed human TRPC7 in the normal extracellular solution that contained 2 mM Ca²⁺ (Figure 5A,B), although the extents of the response, even when they reached the maximum, appeared to be markedly lower than that seen in the TRPC6 cells. Previously, it was shown that extracellular Ca²⁺ potentiated TRPC6 but inhibited TRPC7 currents.⁴¹ Thus, the lower response of TRPC7 to **4o** than TRPC6 reflected at least in part a block by the 2 mM Ca²⁺ included in the

extracellular solution, although such a block may be much weaker than TRPC3, which was almost completely inhibited by the same concentration of Ca^{2+} (see above and Figure 4A). In whole-cell voltage clamp recordings, **4o** elicited concentration dependent current increases in the TRPC7 cells (Figure 5D). Different from TRPC6, the currents showed some desensitization in the high **4o** concentrations (10 and 30 μM) at both negative and positive potentials even though the low Ca^{2+} (0.1 mM) bath solution was used. Nonetheless, a stepwise increase in the TRPC7 currents was still detected at $<10 \mu\text{M}$ **4o**. On the basis of the whole-cell recordings performed in the low Ca^{2+} bath solution, **4o** had an estimated EC_{50} of $1.13 \pm 0.03 \mu\text{M}$ ($n = 6$) on TRPC7. This value is only slightly higher than that obtained from the Ca^{2+} assay. On the basis of the Ca^{2+} assay, the EC_{50} values of **4m–4p** were estimated to be 213 ± 36 , 90 ± 12 , 497 ± 91 , and 314 ± 59 nM (Figure 5C, $n = 6$ for each), respectively. For each of the compounds, the EC_{50} value for TRPC7 is in between those for TRPC3 and TRPC6 (Table 2).

The above data clearly demonstrate the agonistic activity of the pyrazolopyrimidine compounds **4m–4p** on the TRPC3/6/7 subgroup of TRPC channels. To verify the selectivity, we tested the effects of **4m–4p** on a number of related TRP channels, including TRPC4, TRPC5, TRPA1, TRPV1, TRPV3, TRPV4, TRPM5, and TRPM8, using either the FMP or Ca^{2+} assay. All compounds were applied at 33 μM when tested for stimulatory activity, which revealed no obvious effect (data not shown). Then the channels were stimulated with their corresponding agonists in the absence or presence of 22 μM **4m–4p**. For most channels, the compounds did not significantly alter the agonist-evoked responses, except for TRPC4, where **4n** and **4p** suppressed the MOR agonist DAMGO-evoked membrane depolarization by ~33% and 13%, respectively, and for TRPM8, where **4n**, **4o**, and **4p** suppressed the menthol-evoked $[\text{Ca}^{2+}]_i$ increase by ~17%, 22%, and 35%, respectively (Figure 6). A small (<20%) inhibition by **4n** was also detected for TRPA1, TRPV1, and TRPM5 (Figure 6).

Finally, we evaluated the ability of compound **4p** to elicit $[\text{Ca}^{2+}]_i$ rise in rat primary glomerular mesangial cells, which endogenously express functional TRPC3/6 channels.^{42,43} **4p** (1 μM) evoked marked increases in $[\text{Ca}^{2+}]_i$, as revealed by the elevation in Fluo-4 fluorescence (Figure 7A). These activities were abolished by 2-aminoethoxydiphenyl borate (2-APB, 30 μM), a nonspecific TRP modulator that inhibits TRPC channels.^{7,37}

CONCLUSIONS

Pharmacological tool compounds play a vital role in drug development and functional characterization of TRPC channels. Using HTS and SAR studies, we have identified a series of potent and direct agonists of TRPC3/6/7 channels. Four of them, compounds **4m–4p**, were further characterized and shown a potency order of TRPC3 > C7 > C6, with **4n** being the most potent with an EC_{50} value of <20 nM on TRPC3. Importantly, these compounds exhibited no stimulatory activity on related TRPC channels, including the subfamily members TRPC4 and C5. Although not directly tested, it is unlikely that compounds **4m–4p** would activate other Ca^{2+} permeable channels endogenously expressed in HEK293 cells such as inositol 1,4,5-trisphosphate receptors and Orai1 or inhibit the sarco/endoplasmic reticulum Ca^{2+} -ATPase as they did not elicit detectable $[\text{Ca}^{2+}]_i$ in parental HEK293 cells

and a number of stable cell lines. A few compounds exhibited weak inhibition on TRPC4 and TRPM8 at high concentrations. Therefore, they are quite selective for the TRPC3/6/7 subgroup of TRPCs. It remains to be determined if the compounds affect ryanodine receptors or voltage-gated Ca²⁺ channels, which are mainly present in excitable cells. Nevertheless, given the current general lack of good pharmacological agonists for the TRPC channels and our demonstration that they activated native TRPC3/6 channels in rat glomerular mesangial cells, the compounds described here should find excellent use in TRPC channel research. Our results may lead to more potent and specific agonists or antagonists of targeting TRPC channels and facilitate the development of related disease therapeutics.

EXPERIMENTAL SECTION

General Methods

Unless noted otherwise, all reagents and solvents were purchased from commercial suppliers and used without further purification. Melting points were determined on a Yuhua X-5 melting point apparatus. All reactions were performed under an argon atmosphere unless otherwise specified. Reaction progress was monitored using analytical thin-layer chromatography (TLC). The purification of all compounds was processed by silica gel column chromatography. ¹H and ¹³C NMR spectra were recorded on a Bruker AV400 spectrometer (400 MHz, ¹H NMR; 101 MHz, ¹³C NMR) at room temperature (rt). NMR spectra were calibrated to the solvent signals of CDCl₃ (δ 7.26 and 77.16 ppm), CD₃OD (δ 3.31 and 49.00 ppm), or DMSO-*d*₆ (δ 2.50 and 39.52 ppm). The chemical shifts are provided in ppm and the coupling constants in Hz. The following abbreviations for multiplicities are used: s, singlet; d, doublet; dd, double doublet; ddd, triple doublet; t, triplet; dt, double triplet; q, quadruplet; m, multiplet; and br, broad. High-resolution MS was carried out with a Thermo LTQ XL Orbitrap instrument. The yield of all compounds for biological testing was determined by HPLC analysis, confirming >95% purity.

General Procedure for the Synthesis of 4a, 4c, 4d, 4f, 4i, 4j, and 4k—To a solution of **13** (1 equiv) in DMF were added appropriate carboxylic acid (1.2 equiv), HOBT (3 equiv), and HBTU (3 equiv). Diisopropyl ethyl amine (9 equiv) was added 15 min later. The reaction was stirred for 5–24 h, quenched with water, diluted with EtOAc, and then washed with water. The organic layer was dried over anhydrous MgSO₄ and the solvent evaporated under reduced pressure. The residue was purified by silica gel column chromatography (CH₂Cl₂:MeOH = 100:1–40:1) to obtain the title compound.

General Procedure⁴⁴ for the Synthesis of 4b, 4e, 4g, and 4h—To a solution of **13** (1 equiv) in CH₂Cl₂ was added appropriate acyl chloride or anhydride. Et₃N (1.2 equiv) was added, and the reaction was stirred at rt for 4–8 h. After removing the solvent, the title compound was purified by silica gel column chromatography (CH₂Cl₂:MeOH = 100:1–40:1).

General Procedure for the Synthesis of 4l–4p—Compound **4l–4p** were synthesized according to the general procedure for the synthesis of **12** (see later).

(6-Bromopyridin-3-yl)(4-(3-(4-fluorophenyl)-7-hydroxy-2-methyl-pyrazolo[1,5-a]pyrimidin-5-yl)piperidin-1-yl) methanone (4a).⁴⁴: The title compound was isolated as a white solid in 83% yield. ¹H NMR (400 MHz, DMSO-*d*₆) δ 11.70 (s, 1H), 8.48 (d, *J* = 2.3 Hz, 1H), 7.84 (dd, *J* = 8.2, 2.2 Hz, 1H), 7.75 (d, *J* = 8.1 Hz, 1H), 7.47–7.44 (m, 2H), 7.30 (t, *J* = 8.8 Hz, 2H), 5.67 (s, 1H), 4.61 (d, *J* = 10.8 Hz, 1H), 3.62 (d, *J* = 11.1 Hz, 1H), 3.13 (s, 1H), 2.91 (t, *J* = 11.4 Hz, 1H), 2.78 (s, 1H), 2.25 (s, 3H), 1.98 (d, *J* = 5.2 Hz, 1H), 1.79 (s, 1H), 1.69 (d, *J* = 9.0 Hz, 2H). ¹³C NMR (101 MHz, DMSO-*d*₆) δ 165.7, 162.4, 160.0, 156.2, 150.0, 148.4, 142.1, 138.0, 131.7, 131.6, 131.5, 128.1, 115.6, 115.4, 102.2, 92.8, 47.3, 41.7, 30.6, 13.0. HRMS (ESI) calcd for C₂₄H₂₂BrFN₅O₂ [M + H]⁺ 510.0941, found 510.0960.

3-(4-Fluorophenyl)-5-(1-((4-methoxyphenyl)sulfonyl)-4-methyl-piperidin-4-yl)-2-methylpyrazolo[1,5-a]pyrimidin-7-ol (4b).⁴⁴: The title compound was isolated as a white solid in 60% yield; mp decomposition. ¹H NMR (400 MHz, DMSO-*d*₆) δ 10.99 (s, 1H), 7.68 (d, *J* = 8.6 Hz, 2H), 7.38 (m, 2H), 7.27 (dd, *J* = 8.7, 6.7 Hz, 2H), 7.12 (d, *J* = 8.5 Hz, 2H), 5.62 (s, 1H), 3.82 (s, 3H), 2.97 (d, *J* = 10.8 Hz, 4H), 2.19 (m, 5H), 1.77 (d, *J* = 4.5 Hz, 2H), 1.17 (s, 3H). ¹³C NMR (101 MHz, DMSO-*d*₆) δ 162.6, 158.1, 155.8, 142.8, 131.7, 131.7, 129.6, 127.4, 127.4, 127.3, 115.4, 115.2, 114.5, 93.7, 55.7, 42.2, 36.5, 33.6, 24.7, 13.0. HRMS (ESI) calcd for C₂₆H₂₈FN₄O₄S [M + H]⁺ 511.1815, found 511.1803

1-(4-(3-(4-Fluorophenyl)-7-hydroxy-2-methylpyrazolo[1,5-a]-pyrimidin-5-yl)-4-methylpiperidin-1-yl)propan-1-one (4c).⁴⁴: The title compound was isolated as a gray solid in 73% yield; mp decomposition. ¹H NMR (400 MHz, CD₃OD) δ 7.45 (s, 2H), 7.21 (s, 2H), 5.36–5.33 (m, 1H), 4.65 (s, 2H), 3.60 (s, 2H), 2.43–2.39 (m, 2H), 2.32 (s, 3H), 2.04 (s, 2H), 1.76 (s, 2H), 1.39 (s, 3H), 1.11 (t, *J* = 7.5 Hz, 3H). ¹³C NMR (101 MHz, DMSO-*d*₆) δ 171.2, 162.5, 160.1, 158.9, 156.1, 150.7, 138.9, 131.8, 127.5, 115.5, 115.3, 102.6, 93.6, 41.1, 37.4, 34.8, 34.1, 25.6, 24.3, 13.1, 9.5. HRMS (ESI) calcd for C₂₂H₂₆FN₄O₂ [M + H]⁺ 397.2040, found 397.2053.

1-(4-(3-(4-Fluorophenyl)-7-hydroxy-2-methylpyrazolo[1,5-a]-pyrimidin-5-yl)-4-methylpiperidin-1-yl)-2,2-dimethyl-propan-1-one (4d).⁴⁴: The title compound was isolated as a yellow solid in 55% yield; mp 203–206 °C. ¹H NMR (400 MHz, CD₃OD) δ 7.42 (s, 2H), 7.20 (s, 2H), 5.87 (s, 0.5H), 5.34 (s, 0.5H), 4.65 (s, 1H), 3.71 (s, 3H), 2.30 (s, 3H), 2.10 (s, 2H), 1.78 (d, *J* = 12.7 Hz, 2H), 1.40 (s, 3H), 1.27 (s, 9H). HRMS (ESI) calcd for C₂₄H₃₀FN₄O₂ [M + H]⁺ 425.2353, found 425.2351.

5-(1-((2,6-Difluorophenyl)sulfonyl)-4-methylpiperidin-4-yl)-2-methyl-3-(4-nitrophenyl)pyrazolo[1,5-a]pyrimidin-7-ol (4e).⁴⁴: The title compound was isolated as an orange solid in 67% yield; mp 224–227 °C. ¹H NMR (400 MHz, DMSO-*d*₆) δ 9.74 (s, 1H), 8.23 (d, *J* = 8.9 Hz, 3H), 7.65–7.57 (m, 2H), 7.22 (t, *J* = 9.1 Hz, 2H), 5.74 (d, *J* = 28.9 Hz, 1H), 2.96 (t, *J* = 9.7 Hz, 2H), 2.56 (s, 2H), 2.41–2.34 (m, 3H), 1.70 (s, 2H), 1.23 (s, 2H), 1.18 (s, 3H). ¹³C NMR (101 MHz, DMSO-*d*₆) δ 169.6, 160.0, 157.5, 145.1, 143.7, 140.7, 137.8, 135.9, 128.4, 123.7, 113.8, 113.8, 113.5, 113.5, 112.1, 112.1, 93.2, 45.7, 42.9, 35.2, 22.7, 10.8, 9.0. HRMS (ESI) calcd for C₂₅H₂₄F₂N₅O₅S [M + H]⁺ 544.1466, found 544.1461.

2-(3,4-Dimethoxyphenyl)-1-(4-(7-hydroxy-2-methyl-3-(4-nitro-phenyl)pyrazolo[1,5-a]pyrimidin-5-yl)-4-methyl-piperidin-1-yl)-ethan-1-one (4f).⁴⁴: The title compound was isolated as an orange solid in 58% yield; mp 113–116 °C. ¹H NMR (400 MHz, DMSO-*d*₆) δ 11.95 (s, 1H), 8.20 (s, 4H), 6.82–6.80 (m, 2H), 6.71 (d, *J* = 8.1 Hz, 1H), 5.85 (d, *J* = 8.1 Hz, 1H), 3.78 (d, *J* = 6.5 Hz, 1H), 3.66 (d, *J* = 5.7 Hz, 6H), 3.60 (s, 2H), 3.30 (d, *J* = 10.5 Hz, 2H), 3.17 (d, *J* = 9.5 Hz, 1H), 2.54 (s, 2H), 2.16 (s, 2H), 1.45 (d, *J* = 39.3 Hz, 2H), 1.21 (s, 1H), 1.18 (s, 3H). ¹³C NMR (101 MHz, DMSO-*d*₆) δ 168.8, 158.0, 149.3, 148.5, 147.3, 129.7, 128.4, 123.7, 120.7, 112.7, 111.8, 55.5, 55.4, 43.0, 40.1, 38.6, 36.3, 35.7, 22.1, 14.0. HRMS (ESI) calcd for C₂₉H₃₂N₅O₆ [M + H]⁺ 546.2353, found 546.2322.

Ethyl 4-(7-Hydroxy-2-methyl-3-(4-nitrophenyl) pyrazolo[1,5-a]-pyrimidin-5-yl)-4-methylpiperidine-1-carboxylate (4g).⁴⁴: The title compound was isolated as an orange solid in 76% yield; mp 174–178 °C. ¹H NMR (400 MHz, DMSO-*d*₆) δ 8.20 (s, 4H), 5.73 (s, 1H), 3.97 (q, *J* = 6.9 Hz, 2H), 3.57 (d, *J* = 12.4 Hz, 2H), 3.16 (s, 2H), 2.54 (s, 3H), 2.19 (s, 2H), 1.51 (s, 2H), 1.18 (s, 3H), 1.13 (t, *J* = 7.0 Hz, 3H). ¹³C NMR (101 MHz, DMSO-*d*₆) δ 154.7, 123.7, 60.5, 40.8, 35.7, 28.8, 14.7. HRMS (ESI) calcd for C₂₂H₂₆N₅O₅ [M + H]⁺ 440.1934, found 440.1931.

tert-Butyl 4-(3-(4-Fluorophenyl)-7-hydroxy-2-methylpyrazolo-[1,5-a]pyrimidin-5-yl)-4-methylpiperidine-1-carboxylate (4h).⁴⁴: The title compound was isolated as a white solid in 62% yield; mp decomposition. ¹H NMR (400 MHz, CDCl₃) δ 8.92 (s, 1H), 7.21 (dd, *J* = 8.0, 5.5 Hz, 2H), 7.04 (t, *J* = 8.5 Hz, 2H), 5.75 (s, 1H), 3.60–3.55 (m, 2H), 3.42–3.37 (m, 2H), 2.26 (s, 3H), 2.02–1.98 (m, 2H), 1.73 (s, 2H), 1.44 (s, 9H), 1.41 (s, 3H). ¹³C NMR (101 MHz, CDCl₃) δ 163.1, 160.7, 157.7, 157.0, 154.8, 151.7, 138.2, 130.7, 130.6, 127.1, 116.3, 116.1, 105.3, 103.1, 95.1, 80.2, 37.4, 28.5, 25.4, 13.1, 1.2, 0.13. HRMS (ESI) calcd for C₂₄H₃₀FN₄O₃ [M + H]⁺ 441.2302, found 441.2310.

Ethyl 4-(7-Hydroxy-2-methyl-3-(4-nitrophenyl)pyrazolo[1,5-a]-pyrimidin-5-yl)piperidine-1-carboxylate (4i).⁴⁴: The title compound was isolated as a yellow solid in 61% yield; mp decomposition. ¹H NMR (400 MHz, CDCl₃) δ 11.37 (s, 1H), 8.05 (d, *J* = 8.7 Hz, 2H), 7.45 (d, *J* = 8.6 Hz, 2H), 5.65 (s, 1H), 4.30 (d, *J* = 10.9 Hz, 2H), 4.12 (q, *J* = 7.1 Hz, 2H), 2.95 (t, *J* = 12.1 Hz, 1H), 2.80 (s, 2H), 2.31 (s, 3H), 2.06–2.04 (m, 2H), 1.67 (ddd, *J* = 25.3, 12.7, 4.3 Hz, 2H), 1.27 (t, *J* = 7.1 Hz, 3H). ¹³C NMR (101 MHz, CDCl₃) δ 157.9, 157.3, 155.4, 151.0, 145.9, 139.3, 138.4, 130.1, 123.3, 102.6, 94.1, 61.7, 43.9, 40.3, 30.7, 14.8, 13.2. HRMS (ESI) calcd for C₂₁H₂₄N₅O₅ [M + H]⁺ 426.1777, found 426.1771.

1-(4-(3-(4-Fluorophenyl)-7-hydroxy-2-methylpyrazolo[1,5-a]-pyrimidin-5-yl)piperidin-1-yl)propan-1-one (4j).⁴⁴: The title compound was isolated as a white solid in 85% yield; mp 164–166 °C. ¹H NMR (400 MHz, CD₃OD) δ 7.51 (s, 2H), 7.17 (s, 2H), 5.80 (s, 1H), 4.67 (d, *J* = 15.8 Hz, 2H), 4.08 (d, *J* = 11.4 Hz, 1H), 3.16 (t, *J* = 12.2 Hz, 1H), 2.87 (s, 1H), 2.67 (d, *J* = 11.0 Hz, 1H), 2.45 (d, *J* = 7.0 Hz, 2H), 2.32 (s, 3H), 1.99 (t, *J* = 15.4 Hz, 2H), 1.75–1.63 (m, 2H), 1.14 (t, *J* = 7.2 Hz, 3H). ¹³C NMR (101 MHz, CD₃OD) δ 174.7, 164.8, 162.3, 159.2, 153.0, 140.3, 133.0, 132.9, 127.9, 116.6, 116.4, 104.7, 93.9, 46.6, 42.8, 41.1, 32.3, 31.9, 27.3, 12.9, 10.0. HRMS (ESI) calcd for C₂₁H₂₄FN₄O₂ [M + H]⁺ 383.1883, found 383.1876.

1-(4-(3-(4-Fluorophenyl)-7-hydroxy-2-methylpyrazolo[1,5-a]pyrimidin-5-yl)piperidin-1-yl)-2,2-dimethylpropan-1-one (4k).⁴⁴: The title compound was isolated as a white solid in 85% yield; mp 267–270 °C. ¹H NMR (400 MHz, DMSO-*d*₆) δ 11.71 (s, 1H), 7.43 (dd, *J* = 8.5, 5.6 Hz, 2H), 7.30 (t, *J* = 8.8 Hz, 2H), 5.59 (s, 1H), 4.41 (d, *J* = 13.3 Hz, 2H), 2.90–2.84 (m, 1H), 2.75 (dd, *J* = 20.8, 8.0 Hz, 2H), 2.23 (s, 3H), 1.89 (d, *J* = 12.2 Hz, 2H), 1.50 (qd, *J* = 12.5, 3.3 Hz, 2H), 1.19 (s, 9H). ¹³C NMR (101 MHz, DMSO-*d*₆) δ 175.1, 162.6, 160.2, 157.3, 156.3, 150.3, 138.8, 131.8, 131.7, 127.2, 127.1, 115.8, 115.5, 102.3, 92.8, 44.8, 38.3, 30.9, 30.8, 28.3, 13.1. HRMS (ESI) calcd for C₂₃H₂₈FN₄O₂ [M + H]⁺ 411.2196, found 411.2170.

tert-Butyl 4-(3-(4-Chlorophenyl)-7-hydroxy-2-methylpyrazolo-[1,5-a]pyrimidin-5-yl)piperidine-1-carboxylate (4l).⁴⁴: The title compound was isolated as a white solid in 82% yield; mp 119–123 °C. ¹H NMR (400 MHz, CDCl₃) δ 11.35 (s, 1H), 7.17 (d, *J* = 8.2 Hz, 2H), 7.09 (d, *J* = 8.1 Hz, 2H), 5.51 (s, 1H), 4.22 (s, 2H), 3.07 (t, *J* = 11.7 Hz, 1H), 2.74 (s, 2H), 2.16 (s, 3H), 2.09 (d, *J* = 12.0 Hz, 2H), 1.62 (dt, *J* = 12.2, 8.7 Hz, 2H), 1.45 (s, 9H). ¹³C NMR (101 MHz, DMSO-*d*₆) δ 157.6, 156.5, 154.2, 150.4, 139.1, 132.0, 131.8, 130.1, 129.1, 102.4, 93.3, 79.2, 30.7, 28.5, 13.4. HRMS (ESI) calcd for C₂₃H₂₈ClN₄O₃ [M + H]⁺ 443.1850, found 443.1832.

Benzyl 4-(3-(4-Chlorophenyl)-7-hydroxy-2-methylpyrazolo[1,5-a]pyrimidin-5-yl)piperidine-1-carboxylate (4m).⁴⁴: The title compound was isolated as a white solid in 85% yield; mp 236–239 °C. ¹H NMR (400 MHz, CD₃OD) δ 7.69–7.66 (m, 2H), 7.39–7.31 (m, 7H), 5.68 (s, 1H), 5.15 (s, 2H), 4.27 (d, *J* = 13.3 Hz, 2H), 2.94 (s, 2H), 2.70–2.67 (m, 1H), 2.48 (s, 3H), 1.93 (d, *J* = 9.3 Hz, 2H), 1.71 (tt, *J* = 12.5, 6.3 Hz, 2H). ¹³C NMR (101 MHz, CD₃OD) δ 168.0, 161.4, 156.9, 150.5, 150.2, 138.2, 134.6, 131.4, 131.1, 129.5, 129.1, 129.0, 128.8, 105.0, 91.2, 68.2, 45.5, 45.2, 32.7, 14.5. HRMS (ESI) calcd for C₂₆H₂₆ClN₄O₃ [M + H]⁺ 477.1693, found 477.1691.

Ethyl 4-(7-Hydroxy-2-methyl-3-(4-(trifluoromethyl)phenyl)-pyrazolo[1,5-a]pyrimidin-5-yl)piperidine-1-carboxylate (4n).⁴⁴: The title compound was isolated as a white solid in 78% yield; mp 258–261 °C. ¹H NMR (400 MHz, DMSO-*d*₆) δ 11.74 (s, 1H), 7.85–7.81 (m, 2H), 7.68–7.66 (m, 2H), 5.64 (s, 1H), 4.06 (dt, *J* = 14.1, 9.2 Hz, 4H), 2.78 (t, *J* = 11.8 Hz, 3H), 2.30 (s, 3H), 1.85 (d, *J* = 12.4 Hz, 2H), 1.56 (tt, *J* = 12.4, 6.3 Hz, 2H), 1.18 (t, *J* = 7.1 Hz, 3H). ¹³C NMR (101 MHz, DMSO-*d*₆) δ 157.2, 156.0, 154.5, 150.0, 139.0, 135.3, 130.2, 125.5, 125.4, 101.9, 93.3, 60.7, 43.4, 30.2, 14.6, 13.1. HRMS (ESI) calcd for C₂₂H₂₄F₃N₄O₃ [M + H]⁺ 449.1801, found 449.1792.

Ethyl 4-(3-(4-Fluorophenyl)-7-hydroxy-2-methylpyrazolo[1,5-a]pyrimidin-5-yl)piperidine-1-carboxylate (4o).⁴⁴: The title compound was isolated as a white solid in 87% yield; mp 241–244 °C. ¹H NMR (400 MHz, CDCl₃) δ 12.12 (s, 1H), 7.14 (dd, *J* = 8.5, 5.4 Hz, 2H), 6.74 (t, *J* = 8.7 Hz, 2H), 5.48 (s, 1H), 4.26 (s, 2H), 4.09 (q, *J* = 7.1 Hz, 3H), 3.20 (t, *J* = 11.9 Hz, 1H), 2.78 (s, 2H), 2.12 (d, *J* = 9.7 Hz, 6H), 1.64 (dt, *J* = 12.1, 8.7 Hz, 3H), 1.24 (t, *J* = 7.1 Hz, 4H). ¹³C NMR (101 MHz, CDCl₃) δ 160.3, 158.0, 157.7, 155.6, 150.9, 139.0, 131.2, 126.8, 115.0, 114.8, 103.17, 92.9, 61.6, 43.9, 39.8, 31.0, 14.8, 12.8. HRMS (ESI) calcd for C₂₁H₂₄FN₄O₃ [M + H]⁺ 399.1832, found 399.1813.

Benzyl 4-(3-(4-Fluorophenyl)-7-hydroxy-2-methylpyrazolo[1,5-a]pyrimidin-5-yl)piperidine-1-carboxylate (4p).⁴⁴: The title compound was isolated as a white solid in 82% yield; mp 206–209 °C. ¹H NMR (400 MHz, DMSO-*d*₆) δ 7.79 (dd, *J* = 8.5, 5.8 Hz, 2H), 7.28 (d, *J* = 4.3 Hz, 4H), 7.23 (dd, *J* = 8.4, 4.0 Hz, 1H), 7.09 (t, *J* = 8.9 Hz, 2H), 5.34 (s, 1H), 5.01 (s, 2H), 4.04 (t, *J* = 12.0 Hz, 2H), 3.09 (d, *J* = 4.9 Hz, 1H), 2.82 (s, 2H), 2.37 (s, 3H), 1.74 (d, *J* = 11.9 Hz, 2H), 1.52 (qd, *J* = 12.6, 3.8 Hz, 2H). ¹³C NMR (101 MHz, DMSO-*d*₆) δ 165.5, 158.6, 158.2, 154.6, 149.0, 147.5, 137.2, 131.7, 128.6, 128.6, 128.5, 127.9, 127.6, 114.8, 114.6, 102.1, 90.3, 66.2, 48.7, 44.0, 43.5, 15.2. HRMS (ESI) calcd for C₂₆H₂₆FN₄O₃ [M + H]⁺ 461.1989, found 461.1984.

General Procedure for the Synthesis of 6a–6c—To a solution of **5** (1 equiv) in water were added NaOH (**6a**, **6c**) (1.2 equiv) or K₂CO₃ (**6b**) (1.2 equiv), appropriate acyl chloride (**6a**, **6c**) (1.2 equiv), or (Boc)₂O (**6b**) (1.2 equiv) dissolved in THF. The mixture was stirred at rt for 5–7 h. The solvent was removed under reduced pressure, and the aqueous phase was adjusted to pH 2 with 1 M HCl. The sample was then extracted with CH₂Cl₂ and dried over anhydrous MgSO₄. The solvent was evaporated under reduced pressure. The residue was used in the next step without further purification.

1-(tert-Butoxycarbonyl)piperidine-4-carboxylic Acid (6a).⁴⁵: The title compound was isolated as a white solid in 90% yield. ¹H NMR (400 MHz, CDCl₃) δ 4.01 (s, 2H), 2.85 (t, *J* = 11.7 Hz, 2H), 2.48 (tt, *J* = 10.9, 3.9 Hz, 1H), 1.90 (d, *J* = 10.9 Hz, 2H), 1.68–1.58 (m, 2H), 1.45 (s, 9H).

1-(Ethoxycarbonyl)piperidine-4-carboxylic Acid (6b).⁴⁶: The title compound was isolated as a white solid in 91% yield. ¹H NMR (400 MHz, CDCl₃) δ 11.01 (s, 1H), 4.14–4.05 (m, 4H), 2.90 (t, *J* = 10.8 Hz, 2H), 2.49 (tt, *J* = 10.9, 3.8 Hz, 1H), 1.91 (d, *J* = 11.9 Hz, 2H), 1.64 (qd, *J* = 11.5, 4.1 Hz, 2H), 1.24 (t, *J* = 7.1 Hz, 3H).

1-((Benzyloxy)carbonyl)piperidine-4-carboxylic Acid (6c).⁴⁷: The title compound was isolated as a white solid in 95% yield. ¹H NMR (400 MHz, CDCl₃) δ 10.72 (s, 1H), 7.39–7.29 (m, 5H), 5.13 (s, 2H), 4.10 (s, 2H), 2.95 (s, 2H), 2.51 (tt, *J* = 10.7, 3.8 Hz, 1H), 1.93 (s, 2H), 1.67 (d, *J* = 10.3 Hz, 2H).

General Procedure for the Synthesis of 7a–7b—To a solution of diisopropyl amine (6.73 mL, 48 mmol) in THF (145 mL) was added *n*-BuLi (2 M in hexane, 24 mL, 48 mmol) at 0 °C. The reaction was stopped to –78 °C 15 min later. Compound **6** (40 mmol) in THF (60 mL) was added to the above solution and stirred for 1 h. Iodomethane (3.75 mL, 60 mmol) in THF (60 mL) was then added. The reaction was warmed to rt and stirred overnight, quenched with saturated NH₄Cl aqueous solution at 0 °C, and the solvent removed. The sample was extracted with EtOAc (3 × 100 mL). The combined organic layer was washed with brine (100 mL), dried over anhydrous MgSO₄, and solvent evaporated under reduced pressure. The residue was purified by silica gel column chromatography (petroleum ether/ EtOAc, 150:1–50:1) to obtain the title compound.

Diethyl 4-Methylpiperidine-1,4-dicarboxylate (7a).⁴⁶: The title compound was isolated as a light-yellow oil in 87% yield. ¹H NMR (400 MHz, CDCl₃) δ 4.13–4.04 (m, 4H), 3.79 (s,

2H), 2.98 (t, $J = 11.4$ Hz, 2H), 2.03 (d, $J = 13.5$ Hz, 2H), 1.35–1.28 (m, 2H), 1.21 (td, $J = 7.1, 5.5$ Hz, 6H), 1.16 (s, 3H).

1-(tert-Butyl) 4-Ethyl 4-Methylpiperidine-1,4-dicarboxylate (7b).⁴⁸: The title compound was isolated as a light-yellow oil in 85% yield. ¹H NMR (400 MHz, CDCl₃) δ 4.17–4.09 (m, 2H), 3.76–3.71 (m, 2H), 2.96 (t, $J = 11.5$ Hz, 2H), 2.04 (d, $J = 13.1$ Hz, 2H), 1.43 (s, 9H), 1.37–1.30 (m, 2H), 1.24 (t, $J = 7.1$ Hz, 3H), 1.18 (s, 3H).

General Procedure for the Synthesis of 8a–8d—To a solution of compound **7** (40 mmol) in THF (10 mL) was added 5 M NaOH (40 mL, 200 mmol) at 0 °C, and the resulting solution was then reacted at 70 °C overnight. After removing the solvent, the sample was diluted with water and extracted with EtOAc (3 × 15 mL). The resulting aqueous phase was adjusted to pH 3 with 1 M HCl and extracted with CH₂Cl₂ for three times, which was then combined with the organic phase and dried over anhydrous MgSO₄. The solvent was removed under reduced pressure. The corresponding carboxylic acid was obtained and used directly in the next step without further purification. Then, to a round-bottom flask with the above carboxylic acid (1 equiv) dissolved in THF was added *N,N'*-carbonyldiimidazole (1.3 equiv) at 0 °C. The resulting solution was stirred at rt for 4 h. To another solution of potassium 3-ethoxy-3-oxopropanoate (1 equiv) in MeCN:THF (1:2) were added MgCl₂ (2 equiv) and 4-dimethylaminopyridine (DMAP, 0.1 equiv) at 0 °C. The resulting solution was stirred at rt for 5 h. The former solution was then added to the latter solution at 0 °C. The resulting mixture was stirred at rt overnight. After removing the solvent and adjusting pH to 4 with 1 M HCl at 0 °C, the product was extracted with EtOAc for three times. The combined organic layer was washed with 1 M HCl, 1 M NaOH, and brine separately, dried over anhydrous MgSO₄, and the solvent removed under reduced pressure to obtain **8** as a yellow oil, which was used directly in the next step without further purification.

Ethyl 4-(3-Ethoxy-3-oxo)propanoyl-4-methylpiperidine-1-carboxylate (8a).⁴⁶: Yield of 82%. ¹H NMR (400 MHz, CDCl₃) δ 4.21–4.15 (m, 2H), 4.10 (q, 2H), 3.62 (s, 2H), 3.51 (s, 2H), 3.35–3.20 (m, 2H), 1.97 (m, 2H), 1.44 (d, $J = 3.7$ Hz, 2H), 1.26 (tt, $J = 10.5, 7.1$ Hz, 6H), 1.18 (s, 3H).

tert-Butyl 4-(3-Ethoxy-3-oxopropanoyl)-4-methylpiperidine-1-carboxylate (8b).⁴⁶: Yield of 86%. ¹H NMR (400 MHz, CDCl₃) δ 4.17 (qd, $J = 7.1, 1.3$ Hz, 2H), 3.53–3.46 (m, 4H), 3.29–3.16 (m, 2H), 1.96–1.91 (m, 2H), 1.42 (s, 11H), 1.29–1.23 (m, 3H), 1.16 (s, 3H).

Benzyl 4-(3-Ethoxy-3-oxopropanoyl)piperidine-1-carboxylate (8c).⁴⁶: Yield of 87%. ¹H NMR (400 MHz, CDCl₃) δ 7.39–7.36 (m, 5H), 5.14 (s, 2H), 4.21 (q, $J = 7.1$ Hz, 4H), 3.51 (s, 2H), 2.89 (d, $J = 10.8$ Hz, 2H), 2.67 (tt, $J = 11.2, 3.7$ Hz, 1H), 1.88 (s, 2H), 1.59 (m, 2H), 1.30 (td, $J = 7.1, 5.6$ Hz, 3H).

tert-Butyl 4-(3-Ethoxy-3-oxopropanoyl) piperidine-1-carboxylate (8d).⁴⁴: Yield of 91%. ¹H NMR (400 MHz, CDCl₃) δ 4.12 (dd, $J = 14.1, 7.0$ Hz, 2H), 4.04 (s, 2H), 3.43 (s, 2H), 2.72 (t, $J = 11.4$ Hz, 2H), 2.59–2.54 (m, 1H), 1.77 (t, $J = 13.6$ Hz, 2H), 1.52–1.43 (m, 2H), 1.38 (s, 9H), 1.22–1.19 (m, 3H).

General Procedure for the Synthesis of 11a–11d—To a sealing tube was added **9** (14.4 mL, 100 mmol), **10** (14.6 mL, 120 mmol), dry CH₂Cl₂ (10 mL) under N₂ atmosphere. The mixture was heated at 100 °C for 24 h. After cooling to rt, the resulting solution was added to a solution of hydrazine hydrochloride (10.3 g, 150 mmol) in EtOH (20 mL) and H₂O (20 mL) in a 250 mL round-bottom flask. The mixture was then heated at 80 °C for 12 h. The resulting solution was concentrated and neutralized with saturated solution of NaHCO₃ to pH 9. The mixture was extracted with EtOAc (3 × 100 mL). The combined organic layer was washed with brine (100 mL), dried over anhydrous MgSO₄, and the solvent removed under reduced pressure. The product was recrystallized with EtOAc to obtain the title compound.

4-(4-Fluorophenyl)-3-methyl-1H-pyrazol-5-amine (11a).⁴⁴: The title compound was isolated as a white solid in 85% yield. ¹H NMR (400 MHz, CDCl₃) δ 7.28–7.24 (m, 2H), 7.07 (t, *J* = 8.7 Hz, 2H), 2.22 (s, 3H).

4-(4-Chlorophenyl)-3-methyl-1H-pyrazol-5-amine (11b).⁴⁴: The title compound was isolated as a white solid in 81% yield. ¹H NMR (400 MHz, CDCl₃) δ 7.35 (d, *J* = 8.4 Hz, 2H), 7.25 (d, *J* = 8.2 Hz, 2H), 2.24 (s, 3H).

3-Methyl-4-(4-(trifluoromethyl) phenyl)-1H-pyrazol-5-amine (11c).⁴⁴: The title compound was isolated as a yellow solid in 88% yield. ¹H NMR (400 MHz, CDCl₃) δ 7.65 (d, *J* = 8.1 Hz, 2H), 7.47 (d, *J* = 8.0 Hz, 2H), 2.31 (d, *J* = 5.5 Hz, 3H).

3-Methyl-4-(4-nitrophenyl)-1H-pyrazol-5-amine (11d).⁴⁴: The title compound was isolated as a yellow solid in 82% yield. ¹H NMR (400 MHz, DMSO-*d*₆) δ 11.76 (s, 1H), 8.21–8.19 (m, 2H), 7.63 (d, *J* = 8.7 Hz, 2H), 4.95 (s, 2H), 2.26 (s, 3H).

General Procedure for the Synthesis of 12—To a solution of **8** (1 equiv) in AcOH was added **11** (1.1 equiv), and the resulting solution was refluxed overnight. After removing the solvent and adjusting pH of the aqueous phase to 8 with a saturated NaHCO₃ solution, the product was extracted with CH₂Cl₂ and dried over anhydrous MgSO₄. The solvent was evaporated under reduced pressure, and the residue was purified by silica gel column chromatography (CH₂Cl₂/MeOH, 100:1–40:1) to obtain compound **12**.

General Procedure for the Synthesis of 13a—To a solution of **12** (R₂ = Boc) in CH₂Cl₂ (3 V/V) was added TFA (V/V) and the mixture stirred at 0 °C for 2 h. After removing the solvent and adjusting pH of the aqueous phase to 8 with a saturated NaHCO₃ solution, the resulting precipitation was filtrated, washed with water, and dried over vacuum. **13a** was obtained and used in the next step without further purification.

General Procedure for the Synthesis of 13b—To a solution of **8** (1 equiv) in EtOH:TFA = (50 mL:10 mL) was added **11a** (1.2 equiv). The resulting solution was stirred at 85 °C, when another 6.5, 8.5, and 25 mL of TFA was added after 10, 20, and 30 h separately. The reaction was quenched with water at 48 h. After removing the solvent and adjusting pH of the aqueous phase to 8 with a saturated NaHCO₃ solution, the product was filtered, the residue washed with water, CH₃OH, and CH₂Cl₂ separately, and then dried over

vacuum to obtain **13b** as a white solid, which was used directly in the next step without further purification.

Cell Lines and Cell Culture

HEK293 cells were grown in DMEM (high glucose) supplemented with 10% heat-inactivated fetal bovine serum (FBS), 100 units/mL penicillin, and 100 $\mu\text{g}/\text{mL}$ streptomycin at 37 °C, 5% CO_2 . Stable cell lines that express human TRPC3, mouse TRPC4, mouse TRPC6, mouse TRPV3, or mouse TRPM8 were established as described previously and maintained in the medium supplemented with G418 (400 $\mu\text{g}/\text{mL}$; Invitrogen).⁴⁹ For those that coexpressed MOR or M5 muscarinic receptor, 100 $\mu\text{g}/\text{mL}$ hygromycin B (Calbiochem) was also included in the culture medium. Stable cell lines that inducibly express human TRPC5, TRPC7, TRPA1, TRPV1, TRPV4, or TRPM5 were established as described previously and maintained in the medium supplemented with 100 $\mu\text{g}/\text{mL}$ hygromycin B and 5 $\mu\text{g}/\text{mL}$ blasticidin.⁵⁰ The expression of TRP channels was induced by the addition of 0.1 μM doxycycline to the culture medium 24 h prior to the assay.

The use of animals was approved by the Animal Experimentation Ethics Committee of Anhui Medical University and in accordance with the guidelines for ethical conduct in the care and use of animals. Glomerular mesangial cells were prepared according to previous report.^{43,51} Briefly, glomeruli were isolated from male Sprague–Dawley rats (260–280 g) using the graded sieving technique. Glomeruli were collected by centrifugation and digested by collagenase (2 mg/mL, Sigma-Aldrich) for 45 min at 37 °C. Following the wash-off of the enzymes, mesangial cells were cultured in RPMI 1640 medium supplemented with 17% FBS, 100 units/mL penicillin G, and 100 $\mu\text{g}/\text{mL}$ streptomycin at 37 °C in a 5% CO_2 humidified incubator.

Fluorescence Ca^{2+} and Membrane Potential Assays

Cells were seeded in wells of 96-well plates precoated with polyornithine at ~100000 cells/well. Cells were loaded with Fluo4-AM (Invitrogen) or Fluo8-AM (TEFLabs) to monitor intracellular Ca^{2+} changes or loaded with the FLIPR Membrane Potential dye (FMP, Molecular Devices) to monitor membrane potential changes with the use of a FlexStation microplate reader (Molecular Devices). The detailed protocols for the FlexStation FMP and Ca^{2+} assays have been described previously.^{37,49,52} Briefly, the extracellular solution for all FlexStation assays contained (in mM): 140 NaCl, 2 CaCl_2 , 1 MgCl_2 , 10 glucose, and 10 HEPES, pH adjusted to 7.4 with NaOH, except for TRPC3 when the 2 CaCl_2 was replaced with 0.5 CaCl_2 . Probenecid (2 mM) was included in all Ca^{2+} assays except for TRPV1. Assays were run at 32 °C.

$[\text{Ca}^{2+}]_i$ measurement in rat mesangial cells was carried out as described previously.⁵³ Briefly, glomerular mesangial cells were seeded on glass coverslips and allowed to grow overnight. In the next day, the cells were loaded with 10 μM Fluo4-AM in the presence of 0.02% pluronic acid F-127 at 37 °C for 1 h in the dark in 1 mM Ca^{2+} saline containing (in mM): 140 NaCl, 5 KCl, 1 CaCl_2 , 1 MgCl_2 , 10 glucose, and 10 HEPES, pH adjusted to 7.4 with NaOH. After washing, the fluorescent signal was measured using a Leica TCS SP5

laser scanning confocal imaging system. The excitation and emission wavelength were 488 and 515 nm, respectively.

For all fluorescence measurement, changes in the fluorescence intensity were displayed as a ratio of fluorescence change to the fluorescence before the application of stimulating compounds (F/F_0).

Electrophysiology Recordings

HEK293 cells stably expressing TRPC channels were seeded in 35 mm dishes at least 5 h before whole-cell patch clamp recordings were performed. Recording pipettes were pulled from micropipette glass (Sutter Instrument) to 2–5 M Ω when filled with a pipet solution containing (in mM): 110 CsCl, 10 HEPES, 10 BAPTA, 1 MgCl₂, 4.77 CaCl₂, pH adjusted to 7.2 with HCl (400 nM free Ca²⁺) and placed in the bath solution containing (in mM): 140 NaCl, 5 KCl, 2 CaCl₂, 1 MgCl₂, 10 glucose, and 10 HEPES, pH 7.4. Individual cells were voltage-clamped in the whole-cell mode using either an EPC9 or EPC10 (HEKA Instruments Inc., Bellmore, NY) amplifier. Voltage commands were made from the PatchMaster program (version 2.60; HEKA), and currents were recorded at 5 kHz. Voltage ramps of 100 ms to –100 mV after a brief (20 ms) step to +100 mV from holding potential of 0 mV were applied every 1 s. Cells were continuously perfused with the bath solution through a gravity-driven multichannel system with the desired channel opening placed about 50 μ m away from the cell being recorded. For some recordings, CaCl₂ in the bath solution was reduced to 0.5 or 0.1 mM as indicated in the figure legends. Drugs were diluted in the bath solution with the desired Ca²⁺ concentration and applied to the cell through perfusion.

Data Analysis

All data were analyzed and plotted using Origin 7.5 (OriginLab) and Graphpad prism (version 5.01). Summary data are presented as the mean \pm SEM. Statistical comparisons were made using Student's *t* test. A *p* value of <0.05 was considered statistically significant.

Supplementary Material

Refer to Web version on PubMed Central for supplementary material.

Acknowledgments

This work was partially supported by grants from NSFC (81573383, 21390402), NSFHP (2014CFB704), IS&TCPC (2015DFA30440, 2014cFB30020), the Applied Basic Research Program of Wuhan Municipal Bureau of Science & Technology, the Applied Basic Research Programs of Scientific and Technologic Council of Suzhou (SYG201521), Natural Science Foundation of Jiangsu Province (BK20160387), Beijing Nova Plan Z (131107000413063), the Fundamental Research Funds for the Central Universities and U.S. National Institutes of Health (NS056942, NS092377, U54 MH084691). We thank Dr. Corey Hopkins for the initial evaluation of the lead compounds.

ABBREVIATIONS USED

[Ca ²⁺] _i	intracellular Ca ²⁺ concentration
Cbz	carboxybenzyl

CCh	carbachol
DAG	diacylglycerols
DAMGO	[D-Ala ² , N-MePhe ⁴ , Gly-ol]-enkephalin
DCM	dichloromethane
EC₅₀	half-maximal stimulation
FBS	fetal bovine serum
FMP	FLIPR membrane potential
HTS	high-throughput screening
MOR	μ opioid receptor
PLC	phospholipase C
PIP₂	phosphatidylinositol 4,5-bisphosphate
SAR	structure–activity relationship
TFA	trifluoroacetic acid
TRPA	transient receptor potential ankyrin
TRPC	transient receptor potential canonical
TRPM	transient receptor potential melatonin
TRPV	transient receptor potential vanilloid

References

1. Putney JW. Physiological mechanisms of TRPC activation. *Pfluegers Arch.* 2005; 451:29–34. [PubMed: 16133266]
2. Kiselyov, K., Lee, KP., Yuan, JP., Muallem, S. Methods to study TRPC channel regulation by interacting proteins. In: Zhu, MX., editor. *TRP Channels*. CRC Press; Boca Raton, FL: 2011. p. 21-43.
3. Sun Y, Sukumaran P, Bandyopadhyay BC, Singh BB. Physiological function and characterization of TRPCs in neurons. *Cells.* 2014; 3:455–475. [PubMed: 24852263]
4. Fu J, Gao Z, Shen B, Zhu MX. Canonical transient receptor potential 4 and its small molecule modulators. *Sci China: Life Sci.* 2015; 58:39–47. [PubMed: 25480324]
5. Feng S, Li H, Tai Y, Huang J, Su Y, Abramowitz J, Zhu MX, Birnbaumer L, Wang Y. Canonical transient receptor potential 3 channels regulate mitochondrial calcium uptake. *Proc Natl Acad Sci U S A.* 2013; 110:11011–11016. [PubMed: 23776229]
6. Tsvilovskyy VV, Zholos AV, Aberle T, Philipp SE, Dietrich A, Zhu MX, Birnbaumer L, Freichel M, Flockerzi V. Deletion of TRPC4 and TRPC6 in mice impairs smooth muscle contraction and intestinal motility in vivo. *Gastroenterology.* 2009; 137:1415–1424. [PubMed: 19549525]
7. Urban N, Hill K, Wang L, Kuebler WM, Schaefer M. Novel pharmacological TRPC inhibitors block hypoxia-induced vasoconstriction. *Cell Calcium.* 2012; 51:194–206. [PubMed: 22280812]
8. Winn MP, Conlon PJ, Lynn KL, Farrington MK, Creazzo T, Hawkins AF, Daskalakis N, Kwan SY, Ebersviller S, Burchette JL, Pericak-Vance MA, Howell DN, Vance JM, Rosenberg PB. A mutation

- in the TRPC6 cation channel causes familial focal segmental glomerulosclerosis. *Science*. 2005; 308:1801–1804. [PubMed: 15879175]
9. Reiser J, Polu KR, Möller CC, Kenlan P, Altintas MM, Wei C, Faul C, Herbert S, Villegas I, Avila-Casado C, McGee M, Sugimoto H, Brown D, Kalluri R, Mundel P, Smith PL, Clapham DE, Pollak MR. TRPC6 is a glomerular slit diaphragm-associated channel required for normal renal function. *Nat Genet*. 2005; 37:739–744. [PubMed: 15924139]
 10. Zhou J, Du W, Zhou K, Tai Y, Yao H, Jia Y, Ding Y, Wang Y. Critical role of TRPC6 channels in the formation of excitatory synapses. *Nat Neurosci*. 2008; 11:741–743. [PubMed: 18516035]
 11. Hartmann J, Dragicevic E, Adelsberger H, Henning HA, Sumser M, Abramowitz J, Blum R, Dietrich A, Freichel M, Flockerzi V, Birnbaumer L, Konnerth A. TRPC3 channels are required for synaptic transmission and motor coordination. *Neuron*. 2008; 59:392–398. [PubMed: 18701065]
 12. Davis J, Burr AR, Davis GF, Birnbaumer L, Molkenin JD. A TRPC6-dependent pathway for myofibroblast transdifferentiation and wound healing in vivo. *Dev Cell*. 2012; 23:705–715. [PubMed: 23022034]
 13. Dietrich, A., Gudermann, T. TRPC6: Physiological function and pathophysiological relevance. In: Nilius, B., Flockerzi, VB., editors. *Mammalian Transient Receptor Potential (TRP) Cation Channels; Handbook of Experimental Pharmacology*. Vol. 222. Springer-Verlag; Berlin, Heidelberg: 2014. p. 157-187.
 14. Seo K, Rainer PP, Shalkey Hahn V, Lee D, Jo S, Andersen A, Liu T, Xu X, Willette RN, Lepore JJ, Marino JP Jr, Birnbaumer L, Schnackenberg CG, Kass DA. Combined TRPC3 and TRPC6 blockade by selective small-molecule or genetic deletion inhibits pathological cardiac hypertrophy. *Proc Natl Acad Sci U S A*. 2014; 111:1551–1556. [PubMed: 24453217]
 15. Wang J, Lu R, Yang J, Li H, He Z, Jing N, Wang X, Wang Y. TRPC6 specifically interacts with APP to inhibit its cleavage by γ -secretase and reduce $A\beta$ production. *Nat Commun*. 2015; 6:8876. [PubMed: 26581893]
 16. Riehle M, Büscher AK, Gohlke BO, Kaßmann M, Kolatsi-Joannou M, Bräsen JH, Nagel M, Becker JU, Winyard P, Hoyer PF, Preissner R, Krautwurst D, Gollasch M, Weber S, Harteneck C. TRPC6 G757D Loss-of-function mutation associates with FSGS. *J Am Soc Nephrol*. 2016; 27:2771–2783. [PubMed: 26892346]
 17. Zandi-Nejad K, Eddy AA, Glasscock RJ, Brenner BM. Why is proteinuria an ominous biomarker of progressive kidney disease? *Kidney Int*. 2004; 92:S76–S89.
 18. Lin MJ, Leung GP, Zhang WM, Yang XR, Yip KP, Tse CM, Sham JS. Chronic hypoxia-induced upregulation of store-operated and receptor-operated Ca^{2+} channels in pulmonary arterial smooth muscle cells: a novel mechanism of hypoxic pulmonary hypertension. *Circ Res*. 2004; 95:496–505. [PubMed: 15256480]
 19. Onohara N, Nishida M, Inoue R, Kobayashi H, Sumimoto H, Sato Y, Mori Y, Nagao T, Kurose H. TRPC3 and TRPC6 are essential for angiotensin II-induced cardiac hypertrophy. *EMBO J*. 2006; 25:5305–5316. [PubMed: 17082763]
 20. Yu Y, Fantozzi I, Remillard CV, Landsberg JW, Kunichika N, Platoshyn O, Tigno DD, Thistlethwaite PA, Rubin LJ, Yuan JX. Enhanced expression of transient receptor potential channels in idiopathic pulmonary arterial hypertension. *Proc Natl Acad Sci U S A*. 2004; 101:13861–13866. [PubMed: 15358862]
 21. Yang SL, Cao Q, Zhou KC, Feng YJ, Wang YZ. Transient receptor potential channel C3 contributes to the progression of human ovarian cancer. *Oncogene*. 2009; 28:1320–1328. [PubMed: 19151765]
 22. Ding X, He Z, Shi Y, Wang Q, Wang Y. Targeting TRPC6 channels in oesophageal carcinoma growth. *Expert Opin Ther Targets*. 2010; 14:513–527. [PubMed: 20235901]
 23. Hofmann T, Obukhov AG, Schaefer M, Harteneck C, Gudermann T, Schultz G. Direct activation of human TRPC6 and TRPC3 channels by diacylglycerol. *Nature*. 1999; 397:259–263. [PubMed: 9930701]
 24. Okada T, Inoue R, Yamazaki K, Maeda A, Kurosaki T, Yamakuni T, Tanaka I, Shimizu S, Ikenaka K, Imoto K, Mori Y. Molecular and functional characterization of a novel mouse transient receptor potential protein homologue TRP7. Ca^{2+} -permeable cation channel that is constitutively activated

- and enhanced by stimulation of G protein-coupled receptor. *J Biol Chem.* 1999; 274:27359–27370. [PubMed: 10488066]
25. Xu X, Lozinskaya I, Costell M, Lin Z, Ball JA, Bernard R, Behm DJ, Marino JP, Schnackenberg CG. Characterization of small molecule TRPC3 and TRPC6 agonist and antagonists. *Biophys J.* 2013; 104:454a.
 26. Doleschal B, Primessnig U, Wölkart G, Wolf S, Schernthaner M, Lichtenegger M, Glasnov TN, Kappe CO, Mayer B, Antoons G, Heinzel F, Poteser M, Groschner K. TRPC3 contributes to regulation of cardiac contractility and arrhythmogenesis by dynamic interaction with NCX1. *Cardiovasc Res.* 2015; 106:163–173. [PubMed: 25631581]
 27. Schleifer H, Doleschal B, Lichtenegger M, Oppenrieder R, Derler I, Frischauf I, Glasnov TN, Kappe CO, Romanin C, Groschner K. Novel pyrazole compounds for pharmacological discrimination between receptor-operated and store-operated Ca²⁺ entry pathways. *Br J Pharmacol.* 2012; 167:1712–1722. [PubMed: 22862290]
 28. Washburn DG, Holt DA, Dodson J, McAtee JJ, Terrell LR, Barton L, Manns S, Waszkiewicz A, Pritchard C, Gillie DJ, Morrow DM, Davenport EA, Lozinskaya IM, Guss J, Basilla JB, Negron LK, Klein M, Willette RN, Fries RE, Jensen TC, Xu X, Schnackenberg CG, Marino JP Jr. The discovery of potent blockers of the canonical transient receptor channels TRPC3 and TRPC6 based on an anilino-thiazole pharmacophore. *Bioorg Med Chem Lett.* 2013; 23:4979–4984. [PubMed: 23886683]
 29. Miehe, S., Kleemann, HW., Struebing, C. Use of norgestimate as a selective inhibitor of TRPC3, TRPC6 and TRPC7 ion channels. US Patent. 8,455,469. Jun 4. 2013
 30. Maier T, Follmann M, Hessler G, Kleemann HW, Hachtel S, Fuchs B, Weissmann N, Linz W, Schmidt T, Lohn M, Schroeter K, Wang L, Rutten H, Strubing C. Discovery and pharmacological characterization of a novel potent inhibitor of diacylglycerol-sensitive TRPC cation channels. *Br J Pharmacol.* 2015; 172:3650–3660. [PubMed: 25847402]
 31. Urban N, Wang L, Kwiek S, Rademann J, Kuebler WM, Schaefer M. Identification and Validation of Larixyl Acetate as a Potent TRPC6 Inhibitor. *Mol Pharmacol.* 2016; 89:197–213. [PubMed: 26500253]
 32. Akbulut Y, Gaunt HJ, Muraki K, Ludlow MJ, Amer MS, Bruns A, Vasudev NS, Radtke L, Willot M, Hahn S, Seitz T, Ziegler S, Christmann M, Beech DJ, Waldmann H. (–)-Englerin A is a potent selective activator of TRPC4 and TRPC5 calcium channels. *Angew Chem Int Ed.* 2015; 54:3787–3791.
 33. Richter JM, Schaefer M, Hill K. Riluzole activates TRPC5 channels independently of PLC activity. *Br J Pharmacol.* 2014; 171:158–170. [PubMed: 24117252]
 34. Richter JM, Schaefer M, Hill K. Clemizole hydrochloride is a novel and potent inhibitor of transient receptor potential channel TRPC5. *Mol Pharmacol.* 2014; 86:514–521. [PubMed: 25140002]
 35. Miller M, Shi J, Zhu Y, Kustov M, Tian JB, Stevens A, Wu M, Xu J, Long S, Yang P, Zholos AV, Salovich JM, Weaver CD, Hopkins CR, Lindsley CW, McManus O, Li M, Zhu MX. Identification of ML204, a novel potent antagonist that selectively modulates native TRPC4/C5 ion channels. *J Biol Chem.* 2011; 286:33436–33446. [PubMed: 21795696]
 36. Zhu Y, Lu Y, Qu C, Miller M, Tian J, Thakur DP, Zhu J, Deng Z, Hu X, Wu M, McManus OB, Li M, Hong X, Zhu MX, Luo HR. Identification and optimization of 2-amino-benzimidazole derivatives as novel inhibitors of TRPC4 and TRPC5 channels. *Br J Pharmacol.* 2015; 172:3495–3509. [PubMed: 25816897]
 37. Hu HZ, Gu Q, Wang C, Colton CK, Tang J, Kinoshita-Kawada M, Lee LY, Wood JD, Zhu MX. 2-amino-ethoxydiphenyl borate is a common activator of TRPV1, TRPV2, and TRPV3. *J Biol Chem.* 2004; 279:35741–35748. [PubMed: 15194687]
 38. Harada H, Yamazaki H, Toyotomi Y, Tateishi H, Mine Y, Yoshida N, Kato S. Novel N-1-(1-Substituted 4-piperidinylmethyl)-4-piperidinyl]benzamides as potent colonic prokinetic agents. *Bioorg Med Chem Lett.* 2002; 12:967–970. [PubMed: 11959005]
 39. Brooks DW, Lu LDL, Masamune S. C-Acylation under virtually neutral conditions. *Angew Chem, Int Ed Engl.* 1979; 18:72–74. [PubMed: 105650]

40. Zhu MX, Tang J. TRPC channel interactions with calmodulin and IP3 receptors. *Novartis Found Symp.* 2004; 258:44–58. [PubMed: 15104175]
41. Shi J, Mori E, Mori Y, Mori M, Li J, Ito Y, Inoue R. Multiple regulation by calcium of murine homologues of transient receptor potential proteins TRPC6 and TRPC7 expressed in HEK293 cells. *J Physiol.* 2004; 561:415–432. [PubMed: 15579537]
42. Sours S, Du J, Chu S, Ding M, Zhou XJ, Ma R. Expression of canonical transient receptor potential (TRPC) proteins in human glomerular mesangial cells. *Am J Physiol Renal Physiol.* 2006; 290:1507–1515.
43. Shen B, Kwan HY, Ma X, Wong CO, Du J, Huang Y, Yao X. cAMP activates TRPC6 channels via the phosphatidylinositol 3-kinase (PI3K)-protein kinase B (PKB)-mitogen-activated protein kinase kinase (MEK)-ERK1/2 signaling pathway. *J Biol Chem.* 2011; 286:19439–19445. [PubMed: 21487005]
44. Hong, X., Wang, H., Zhu, X., Ding, M., Lv, G., Zhang, J., Wen, M., Qu, C., Zhu, J., Hu, X. Preparation of pyrazolo[1,5-*a*]pyrimidine derivatives as antitumor agents. *Faming Zhuanli Shenqing.* CN 104292233A. Jan 21. 2015
45. Attardo, G., Breining, T., Courchesne, M., Lamothe, S., Lavallee, JF., Nguyen, D., Rej, R., St-Denis, Y., Wang, W., Xu, Y., Barbeau, F., Lebeau, E., Kraus, J. Antineoplastic heteronaphthoquinones. *US Patent.* 5,736,523. Apr 7. 1998
46. Luo, H., Hong, X., Zhu, X., Zhu, J., Wu, G., Deng, Z., Zhu, Y., Lu, Y., Deng, K., Qu, C. Preparation of pyrazolopyrimidine compounds for treatment of glomerular diseases or myocardial hypertrophy. *Faming Zhuanli Shenqing.* CN 103694242A. Apr 2. 2014
47. Brown GR, Hollinshead DM, Stokes ES, Waterson D, Clarke DS, Foubister AJ, Glossop SC, McTaggart F, Mirrlees DJ, Smith GJ, Wood R. A novel series of 4-piperidinopyridine and 4-piperidinopyrimidine inhibitors of 2, 3-oxidosqualene cyclase–lanosterol synthase. *J Med Chem.* 2000; 43:4964–4972. [PubMed: 11150166]
48. Davies, D., Jones, G., Markwell, R., Pearson, N. Preparation of *N*-(1,5-naphthyridin-4-yl)piperidine-4-carboxamide derivatives as antibacterial agents. *PCT Int Appl WO.* 2003010138A2. Feb 6. 2003
49. Miller, M., Wu, M., Xu, J., Weaver, D., Li, M., Zhu, MX. High-throughput screening of TRPC channel ligands using cell-based assays. In: Zhu, MX., editor. *TRP Channels.* CRC Press; Boca Raton, FL: 2011. p. 1-20.
50. Hu H, Tian J, Zhu Y, Wang C, Xiao R, Herz JM, Wood JD, Zhu MX. Activation of TRPA1 channels by fenamate nonsteroidal anti-inflammatory drugs. *Pfluegers Arch.* 2010; 459:579–592. [PubMed: 19888597]
51. Zhang X, Chen X, Wu D, Liu W, Wang J, Feng Z, Cai G, Fu B, Hong Q, Du J. Downregulation of connexin 43 expression by high glucose induces senescence in glomerular mesangial cells. *J Am Soc Nephrol.* 2006; 17:1532–1542. [PubMed: 16675599]
52. Otsuguro K, Tang J, Tang Y, Xiao R, Freichel M, Tsvilovskyy V, Ito S, Flockerzi V, Zhu MX, Zholos AV. Isoform-specific inhibition of TRPC4 channel by phosphatidylinositol 4, 5-bisphosphate. *J Biol Chem.* 2008; 283:10026–10036. [PubMed: 18230622]
53. Shen B, Cheng KT, Leung YK, Kwok YC, Kwan HY, Wong CO, Chen ZY, Huang Y, Yao X. Epinephrine-induced Ca²⁺ influx in vascular endothelial cells is mediated by CNGA2 channels. *J Mol Cell Cardiol.* 2008; 45:437–445. [PubMed: 18621055]

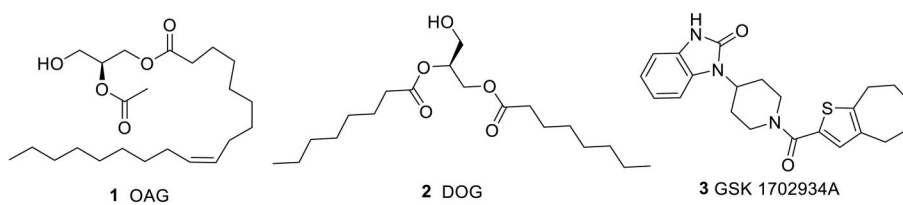


Figure 1.
Examples of reported TRPC3/6/7 agonists.

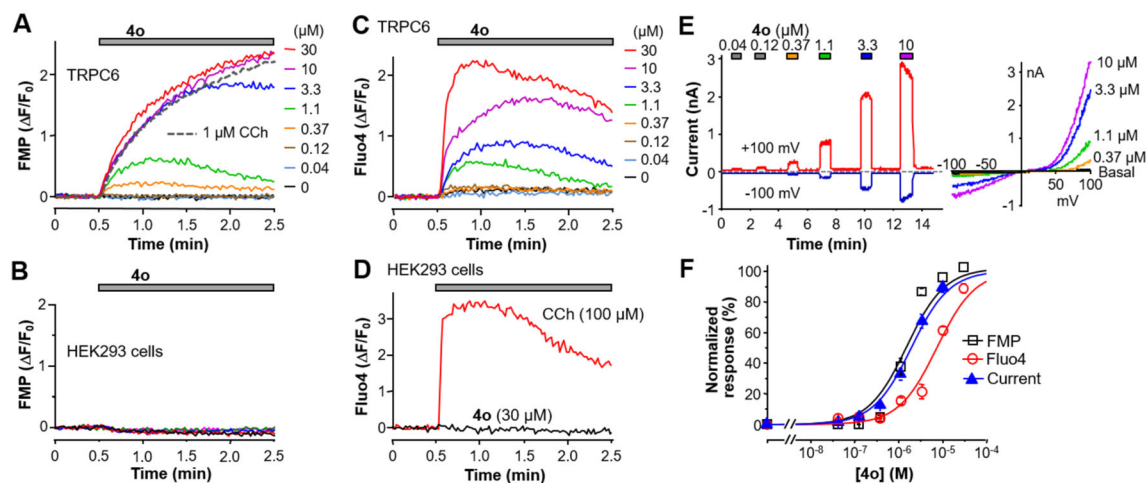


Figure 2.

Lead compound **4o** identified from HTS activated TRPC6 expressed in HEK293 cells. (A) Representative traces of membrane potential changes evoked by carbachol (CCh, 1 μ M, gray dashed line) or varying concentrations of compound **4o** obtained from the compound library (colored lines) in the TRPC6 cells. The fluorescence increases indicate depolarization. (B) Compound **4o** did not induce membrane depolarization in parental HEK293 cells. (C) Representative traces of Fluo4 fluorescence changes, indicative of $[Ca^{2+}]_i$ increase, evoked by varying concentrations of compound **4o** in the TRPC6 cells. (D) CCh, but not compound **4o**, evoked $[Ca^{2+}]_i$ increase in the parental HEK293 cells. (E) Representative traces of whole-cell currents at +100 mV (red trace) and -100 mV (blue trace) elicited by varying concentrations of compound **4o** in a TRPC6 cell. The bath contained 2 mM Ca^{2+} , and the pipet solution had 400 nM free Ca^{2+} buffered by BAPTA. Voltage ramps from +100 mV to -100 mV were applied every second. Current-voltage ($I-V$) relationships obtained from the voltage ramps for peak currents elicited by selected compound concentrations are shown at right. These $I-V$ curves are typical to TRPC6 currents evoked through receptor stimulation.³⁷ (F) Concentration response curves for compound **4o** activation of TRPC6, as determined by the membrane potential assay (FMP), Ca^{2+} assay (Fluo4) and electrophysiology recording shown in A, C, and E, respectively. For fluorescence assays, area under the curve, and for whole-cell recordings, peak current changes at +80 mV were used for quantification. Solid lines represent fits by the Hill equation, which yielded the EC_{50} values described in the text.

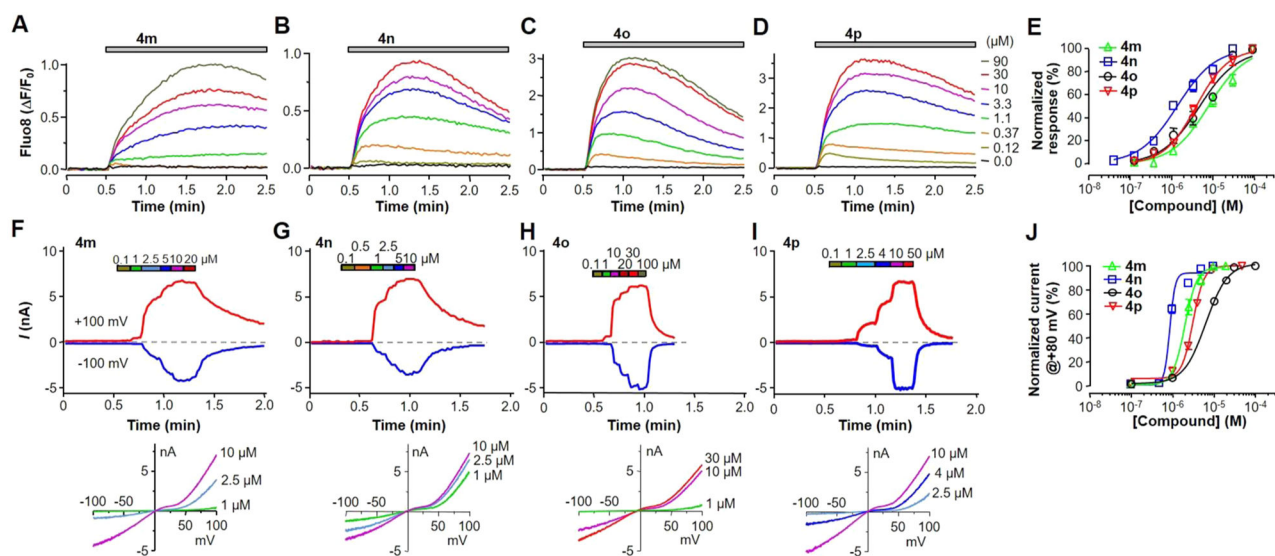


Figure 3.

Compounds **4m–4p** activated TRPC6 expressed in HEK293 cells. (A–E) Compounds **4m–4p** were synthesized as described in the text and tested in the Ca^{2+} assay using Fluo8-loaded TRPC6 cells. (A–D) Representative traces of $[Ca^{2+}]_i$ rise, as indicated by the Fluo8 fluorescence increase, evoked by varying concentrations of **4m** (A), **4n** (B), **4o** (C), or **4p** (D). (E) Summary data for (A–D) and the fits by the Hill equation. (F–J) Compounds **4m–4p** were tested on TRPC6 cells in whole-cell recordings. The bath contained 0.1 mM Ca^{2+} , and the pipet solution had 400 nM free Ca^{2+} buffered by BAPTA. (F–I) Representative current traces at +100 mV (red traces) and -100 mV (blue traces) in response to consecutive applications of increasing concentrations of **4m** (F), **4n** (G), **4o** (H), or **4p** (I) (upper panels) and $I-V$ curves for selected compound concentrations (lower panels). (J) Summary data for (F–I) and the fits by the Hill equation.

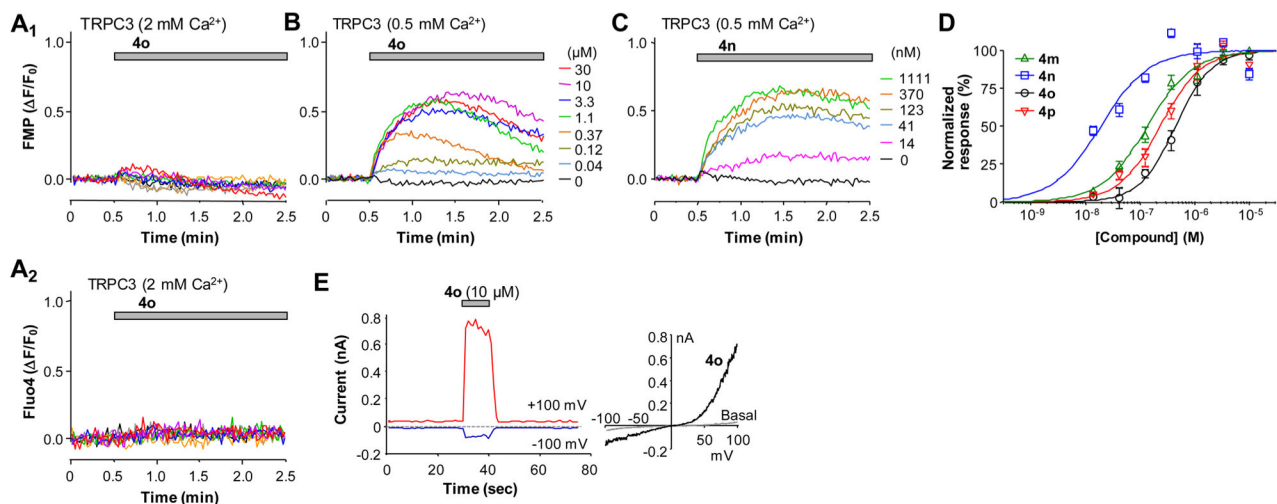


Figure 4.

Compounds **4m–4p** activated TRPC3 expressed in HEK293 cells when extracellular solution contained 0.5 mM Ca^{2+} . (A) Compound **4o** failed to elicit membrane depolarization (A₁) or $[Ca^{2+}]_i$ rise (A₂) in TRPC3 cells in normal extracellular solution that contained 2 mM Ca^{2+} . (B,C) Representative traces of membrane potential depolarization induced by varying concentrations of compounds **4o** (B) and **4n** (C) in TRPC3 cells in an extracellular solution that contained 0.5 mM Ca^{2+} . (D) Summary data for membrane depolarization induced by compounds **4m–4p** in TRPC3 cells bathed in the 0.5 mM Ca^{2+} solution. The data points were fitted by the Hill equation. (E) Compound **4o** (10 μM) elicited TRPC3 currents in the bath that contained 0.5 mM Ca^{2+} . The $I-V$ curves under basal and **4o**-stimulated conditions are shown at right.

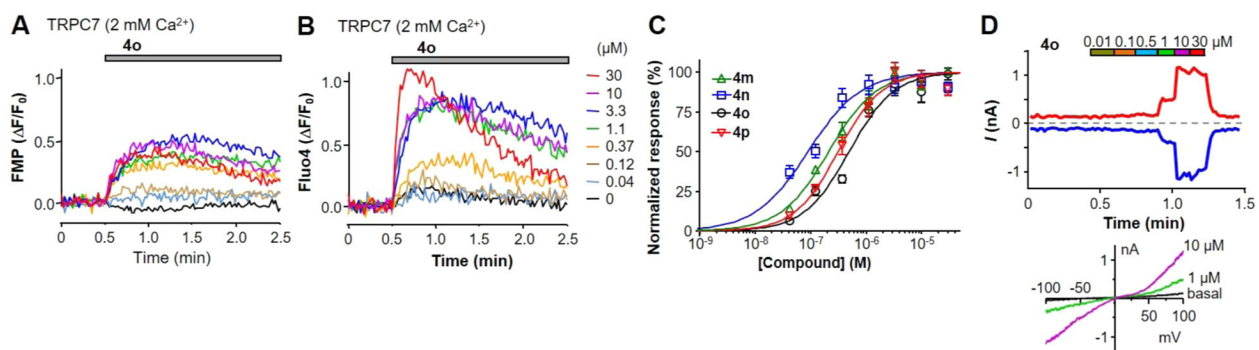


Figure 5.

Compounds **4m–4p** activated TRPC7 expressed in HEK293 cells. (A,B) Representative traces of membrane potential depolarization (A) and $[Ca^{2+}]_i$ increase (B) induced by varying concentrations of compounds **4o** in TRPC7 cells in normal extracellular solution that contained 2 mM Ca^{2+} . (C) Summary data for $[Ca^{2+}]_i$ rise induced by compounds **4m–4p** in TRPC7 cells bathed in the 2 mM Ca^{2+} solution, as exemplified in (B). The data points were fitted by the Hill equation. (D) Activation of TRPC7 currents by increasing concentrations of compound **4o** in the bath solution that contained 0.1 mM Ca^{2+} . The $I-V$ curves under basal and selected concentrations of **4o** are shown below.

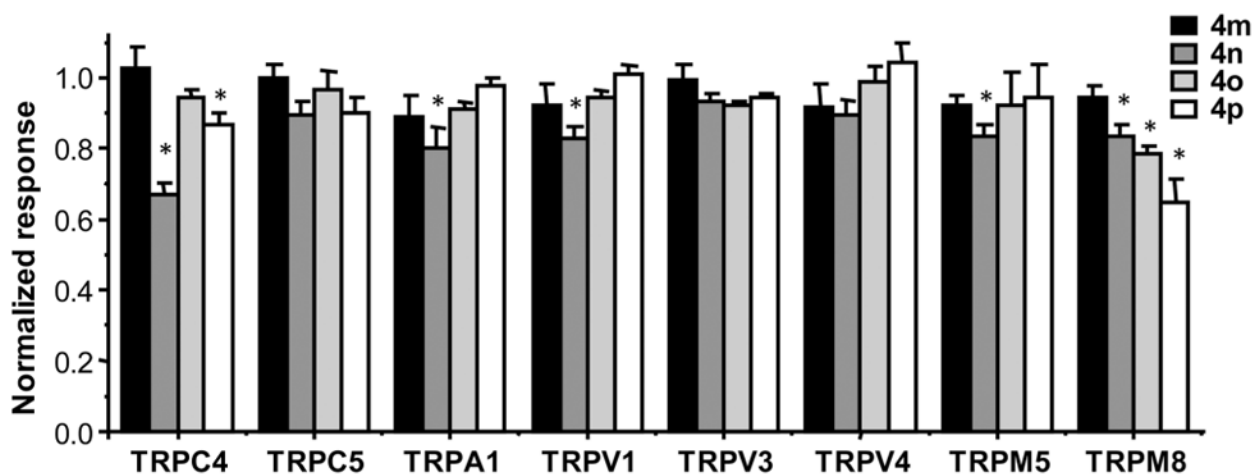


Figure 6.

Compounds **4m–4p** had little or no effect on related TRP channels. Stable HEK293 cell lines expressing MOR/TRPC4 β , TRPC5, TRPA1, TRPV1, TRPV3, TRPV4, TRPM5, and TRPM8 were seeded in wells of 96-well plates and loaded with either FMP dye (TRPC4, C5, and M5) or Fluo8-AM (TRPA1, V1, V3, V4, and M8). Changes in membrane potential or $[Ca^{2+}]_i$ were read in a microplate reader, while compound **4m**, **4n**, **4o**, or **4p** (33 μ M) was applied for 2 min before the corresponding agonist known to activate the channel (C4, 1 μ M DAMGO; C5, 100 μ M CCh; A1, 100 μ M flufenamic acid; V1, 1 μ M capsaicin; V3, 200 μ M 2-APB; V4, 30 μ M RN-1747; M5, 100 μ M CCh; M8, 100 μ M menthol) was added, and measurement continued for 2.5 min. After the agonist addition, the test compound was diluted to 22 μ M. Shown are summary data for the agonist-evoked response (area under the curve) in the presence of the test compound normalized to that in the absence of the test compound. $n = 4–10$ measurements. * $p < 0.05$ compared to no test compound by Student's t test.

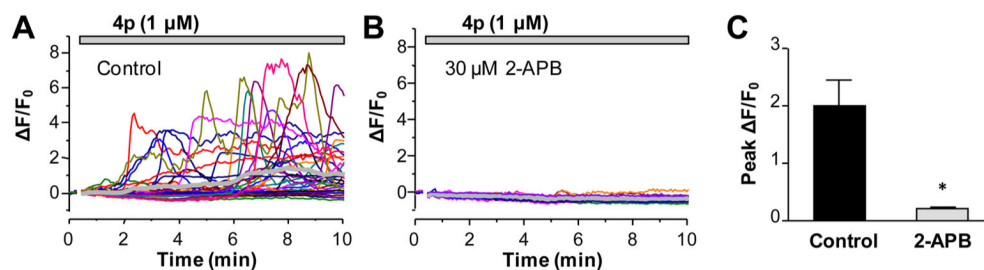
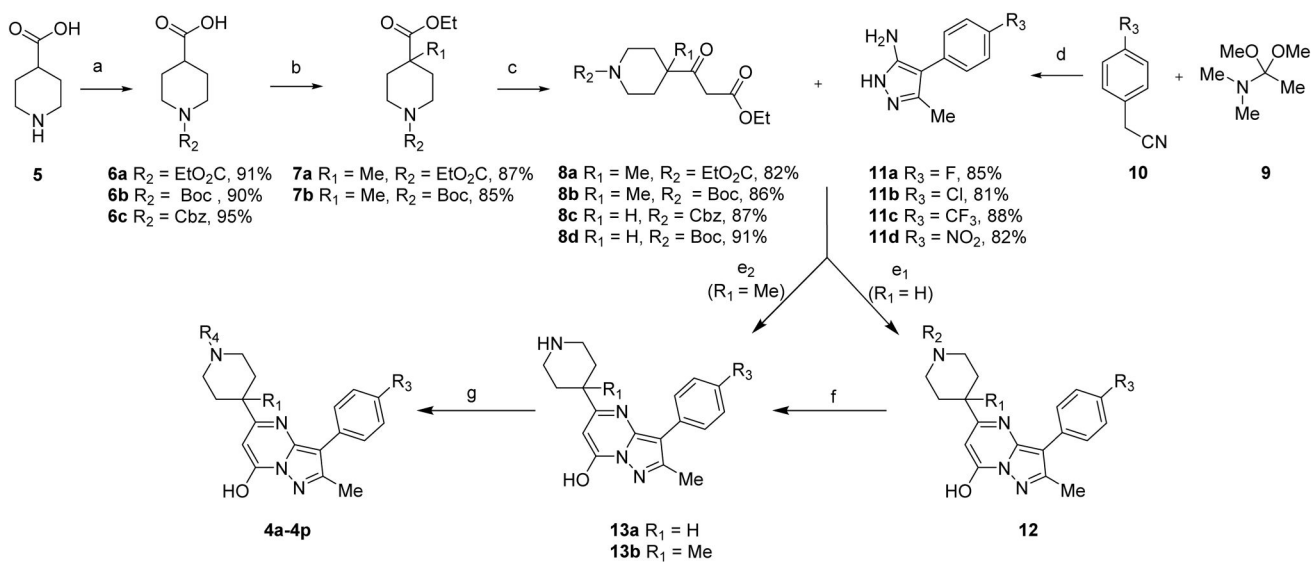


Figure 7.

Compound **4p** induced Ca^{2+} transients in rat glomerular mesangial cells. (A) Representative traces of Fluo4-loaded mesangial cells exposed to $1 \mu\text{M}$ compound **4p**. Each trace represents a single cell, and the thick gray line is the average of all 36 cells in the same coverslip. (B) Similar to (A), but the cells were pretreated for 2 min with $30 \mu\text{M}$ 2-APB, which was also present throughout the period when compound **4p** was applied. Each trace represents a single cell, and the thick gray line is the average of all 30 cells in the same coverslip. (C) Summary of four experiments quantified by the mean peak fluorescence changes induced by compound **4p** for the individual experiments. * $p < 0.05$ compared to no 2-APB control by Student's t test.

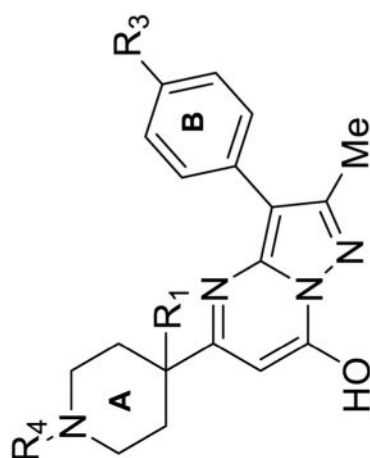


Scheme 1. Synthetic Route for Compound 4a and its Derivatives^a

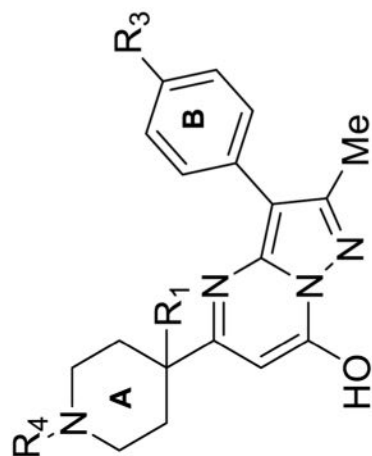
^aReagents and conditions: (a) R₁O₂CCl, NaOH, H₂O, rt, 5 h, or (Boc)₂O, K₂CO₃, THF/H₂O, rt, 7 h; (b) (i) ClCO₂Et, NEt₃, rt, 12 h, (ii) *n*-BuLi, *i*-Pr₂NH, THF, -78 °C, 1 h, MeI, THF, 5 h; (c) (i) 2 M NaOH, (ii) CDI, THF, 4 h, KO₂CCH₂CO₂Et, MgCl₂, DMAP, THF/CH₃CN, overnight; (d) (i) DCM, microwave, 100 °C, (ii) N₂H₄·HCl, H₂O, EtOH, 80 °C, 8 h; (e₁) AcOH, reflux, 120 °C, overnight; (e₂) EtOH, TFA, reflux, 85 °C, 48 h; (f) TFA, DCM, 0 °C, 2 h; (g) DMF, HOBt, HBTU, DIPEA, rt, overnight.

Table 1

Structures of Compounds 4a–4p and Their Effects on TRPC6 and TRPC4

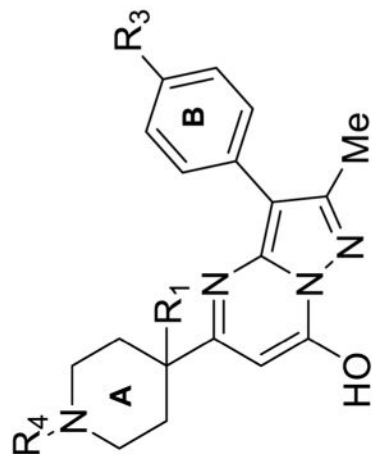
**4a-4p**

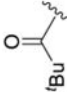
Compound	R ₁	R ₃	R ₄	TRPC6 EC ₅₀ (μ M) ^a	TRPC4+MOR IC ₅₀ (μ M) ^b
4a	H	F		12.3 \pm 1.2	~10
4b	Me	F		NA	NA
4c	Me	F		NA	NA
4d	Me	F		NA	NA



4a-4p

Compound	R ₁	R ₃	R ₄	TRPC6 EC ₅₀ (μ M) ^a	TRPC4 β -MOR IC ₅₀ (μ M) ^b
4e	Me	NO ₂		NA	NA
4f	Me	NO ₂		NA	NA
4g	Me	NO ₂	CO ₂ Et	~8 ^c	NA
4h	Me	F	Boc	NA	NA
4i	H	NO ₂	CO ₂ Et	~2 ^c	NA
4j	H	F		28.8±8.3	~35

**4a-4p**

Compound	R ₁	R ₂	R ₃	R ₄	TRPC6 EC ₅₀ (μ M) ^a	TRPC4 β -MOR IC ₅₀ (μ M) ^b
4k	H	F	F		NA	NA
4l	H	Cl	Cl	Boc	NA	NA
4m	H	Cl	Cl	Cbz	7.79 \pm 0.05	NA
4n	H	CF ₃	CF ₃	CO ₂ Et	1.39 \pm 0.01	NA
4o	H	F	F	CO ₂ Et	4.66 \pm 0.03	NA
4p	H	F	F	Cbz	3.91 \pm 0.02	NA

^aEC₅₀ determined based on Ca²⁺ assay.

^bIC₅₀ against that activated by 1 μ M DAMGO, estimated based on one experiment with triplicates;

^cEstimated value because of the self-fluorescence of the compound.

NA: No activity.

Table 2EC₅₀ Values (μM) for Compounds 4m–4p to TRPC3/6/7 Channels

compd	TRPC3 ^a	TRPC7 ^b	TRPC6 ^b	TRPC6 ^c
4m	0.138 ± 0.023	0.213 ± 0.036	7.79 ± 0.05	2.05 ± 0.02
4n	0.019 ± 0.002	0.090 ± 0.012	1.39 ± 0.01	0.89 ± 0.01
4o	0.450 ± 0.087	0.497 ± 0.091	4.66 ± 0.03	6.28 ± 0.02
4p	0.236 ± 0.047	0.314 ± 0.059	3.91 ± 0.02	3.24 ± 0.01

^aCells were loaded with the FLIPR membrane potential (FMP) blue dye; the $[\text{Ca}^{2+}]$ in the bath was 0.5 mM.

^bCells were loaded with Fluo8-AM; the $[\text{Ca}^{2+}]$ in the bath was 2 mM.

^cDetermined based on currents at +80 mV by whole-cell patch clamp recordings using a bath solution that contained 0.1 mM Ca^{2+} and a peptide solution that contained 400 nM free Ca^{2+} buffered with BAPTA.